

DESIGN AND CONTROL OF A HIGH-EFFICIENCY SYSTEM FOR ELECTRIC AIR
TAXIS USING MPC AND LQR CONTROL, AND GAN-BASED POWER
ELECTRONICS WITH OPTIMIZED LITHIUM-SULFUR BATTERY
MANAGEMENT

by

AHMAD ALI KHAN

A dissertation submitted in partial fulfillment of the
requirements for the degree of

DOCTOR OF PHILOSOPHY IN ELECTRICAL AND COMPUTER ENGINEERING

2024

Oakland University
Rochester, Michigan

Doctoral Advisory Committee:

Mohamed A. Zohdy, Ph.D., Chair

Osamah Rawashdeh, Ph.D.

Darrell Schmidt, Ph.D.

Gary Barber, Ph.D.

© Copyright by Ahmad Ali Khan, 2024
All rights reserved

To my mother and father, my heartfelt gratitude for your unwavering support throughout this doctoral journey. From my earliest days, you instilled in me a tireless work ethic and a deep-seated belief that I could achieve anything I set my mind to. Your refusal to accept anything less than my best pushed me to strive for the extraordinary and your example taught me the value of resilience and determination.

The path to this degree wasn't always easy, yet your presence was a constant source of strength. Knowing you were always there, cheering me on and believing in my abilities, gave me the courage to keep going even when I stumbled. This dissertation serves as a testament to your unwavering love, the sacrifices you've made, and the exceptional foundation you laid for me. Thank you – I wouldn't be here without you.

ACKNOWLEDGMENTS

Firstly, my sincerest gratitude goes to my DAC chair, Dr. Mohamed A. Zohdy, for his mentorship and support throughout my academic journey. His insights, guidance, and unwavering belief in my work were invaluable, pushing me to reach new intellectual heights. I'd also like to thank my esteemed committee members, Dr. Osamah Rawashdeh, Dr. Darrell Schmidt, and Dr. Gary Barber. Their constructive feedback, thoughtful questions, and expertise have immeasurably strengthened my research and this dissertation. A big thank you to Bonnie Koch, who has been extremely supportive during my tenure at Oakland University, dating back to my BSEE. Thank you for all the help, support, and conversations throughout the years. Thank you to Dr. Michel Sultan and Dr. S. Ali Arefifar who were incredible resources early in my academic career.

My journey would have been impossible without the unwavering love and support of my friends and family. To everyone who contributed to my earning of this Ph.D., I extend my deepest gratitude. You know who you are, and this achievement belongs to all of us. Your constant encouragement, unwavering patience, and willingness to be my sounding board were essential to my success. Thank you for celebrating the victories alongside me and helping me overcome all of the challenges.

And to the 18-year-old me, who could never have imagined we'd make it this far, look at us now. Thank you for your patience and unwavering determination. Your hard work truly paid off.

Ahmad Ali Khan

ABSTRACT

DESIGN AND CONTROL OF A HIGH-EFFICIENCY SYSTEM FOR ELECTRIC AIR TAXIS USING MPC AND LQR CONTROL, AND GAN-BASED POWER ELECTRONICS WITH OPTIMIZED LITHIUM-SULFUR BATTERY MANAGEMENT

by

AHMAD ALI KHAN

Adviser: Mohamed A. Zohdy, Ph.D.

Lithium-sulfur (Li-S) batteries are a new type of battery that could revolutionize the way we store energy. They have the potential to deliver much more energy than current lithium-ion batteries, which are used in everything from electric cars to smartphones.

Li-S batteries work by storing lithium ions in sulfur. Sulfur is a very cheap and readily accessible material, so Li-S batteries have the potential to be much cheaper than lithium-ion batteries.

However, some challenges must be addressed before Li-S batteries can be commercialized. One challenge is the shuttle effect. The shuttle effect is a process in which polysulfides (the sulfur compounds that store lithium ions in Li-S batteries) dissolve in the electrolyte and travel to the anode.

Another challenge is the formation of lithium dendrites. Lithium dendrites are needle-like structures that can grow on the surface of the battery's anode.

A key application for Li-S batteries would be in electric air taxis. Electric air taxis are an exciting new technology that has the potential to revolutionize urban transportation. These aircraft are designed to provide fast, efficient, and environmentally friendly transportation for short-to-medium distance trips within urban areas. They are typically smaller and more agile than traditional helicopters or airplanes and can take off and land vertically, which eliminates the need for a runway.

Battery models do not consider specific Li-S battery chemical phenomena – which does not provide an accurate representation of how the battery ages. Furthermore, implementing model predictive control provides an innovative approach to address the dynamic and nonlinear challenges inherent in air taxi flight, offering a sophisticated solution for precise and adaptive thrust control.

This dissertation highlights the modeling of an air taxi, as well as a more accurate representation of the battery as it ages. Introducing the MPC ties together the overall control of the vehicle.

TABLE OF CONTENTS

ACKNOWLEDGMENTS	iv
ABSTRACT	v
LIST OF TABLES	xi
LIST OF FIGURES	xii
LIST OF ABBREVIATIONS	xiv
CHAPTER ONE	
INTRODUCTION	1
1.1 What are Lithium-Sulfur Batteries?	1
1.2 Why are Lithium-Sulfur Batteries Promising?	3
1.3 Challenges and Opportunities for Lithium-Sulfur Batteries	4
1.4 Challenges with Dendrite Growth	6
1.5 Challenges with Polysulfide Shuttle Effect	8
1.6 Challenges with Modeling	10
1.7 MPC vs. LQR Thrust Control	13
1.8 Motivation and Research Goal	14
1.9 Dissertation Contributions	15
CHAPTER TWO	
RELATED WORK	17
2.1 Literature Review	17
2.1.1 Literature Review – Battery	17
2.1.2 Literature Review – Motor	21

TABLE OF CONTENTS—Continued

2.1.3 Literature Review – Power Electronics	22
2.1.4 Literature Review – Controls	24
2.1.5 Strengths of Previous Research	28
2.1.6 Weaknesses of Previous Research	29
CHAPTER THREE	
AIR TAXI SIMULATION UTILIZING MATLAB/SIMULINK	30
3.1 Overall Air Taxi Project	30
3.2 Battery Improvements	30
3.3 Motor Improvements	34
CHAPTER FOUR	
LITHIUM SULFUR BATTERY MODEL SUBSYSTEM	45
4.1 Introduction to Simulink Model	45
4.1.1 Purpose and Significance	45
4.1.2 Brief Overview of the Model's Intent to Represent Dendrite Growth and the Shuttle Effect	46
4.2 Model Development and Configuration	46
4.2.1 Brief Description of Model's Architecture	47
4.2.2 Battery Model	49
4.2.3 Voltage Sensor (V)	49
4.2.4 Controlled Current Sensor (I)	50
4.3 Temperature Mechanism	50

TABLE OF CONTENTS—Continued

4.4 Charging and Discharging Profile Mechanism	53
4.5 Dendrite Growth and Shuttle Effect Representation	55
4.5.1 Aging Model	56
4.6 Simulation Results Model Development and Configuration	58
4.6.1 Voltage Output	58
4.6.2 Capacity	60
4.6.3 Resistance	62
4.7 Comparison with Lab Data	64
4.8 Conclusion	66
CHAPTER FIVE	
MODEL PREDICTIVE CONTROL AND LINEAR QUADRATIC REGULATOR IMPLEMENTATION	68
5.1 Control Design and Simulation	68
5.1.1 System Overview	69
5.1.2 Converter Modeling	71
5.1.3 Motor Modeling	74
5.1.4 MPC Controller Design	78
5.1.5 Comparison with LQR	81
5.1.6 MPC Block Tuning	82
5.2 Simulation and Results	82

TABLE OF CONTENTS—Continued

CHAPTER SIX	
CONCLUSION AND FUTURE WORK	89
6.1 Conclusion	89
6.2 Future Work	90
REFERENCES	91

LIST OF TABLES

Table 1	Air Taxi Dimensions	30
Table 2	Abbreviations of Each Variable	73

LIST OF FIGURES

Figure 3.1	Energy Density by Battery Chemistry	31
Figure 3.2	Weight Comparison Li-ion and Li-S	32
Figure 3.3	Battery Capacity Initial	33
Figure 3.4	Improved Battery Capacity	33
Figure 3.5	Simulink Air Taxi Model	34
Figure 3.6	General Air Taxi Model Range and Flight Time	35
Figure 3.7	Improved Air Taxi Model Range and Flight Time	36
Figure 3.8	Power and Energy with Li-ion Battery	37
Figure 3.9	Power and Energy with Li-Sulfur Battery	37
Figure 3.10	Speed and Height with Li-ion Battery	38
Figure 3.11	Speed and Height with Li-Sulfur Battery	38
Figure 3.12	Range vs. Battery Capacity Li-ion Battery	39
Figure 3.13	Range vs. Battery Capacity Li-Sulfur Battery	40
Figure 3.14	Max Flight Time vs. Battery Capacity Li-ion Battery	41
Figure 3.15	Max Flight Time vs. Battery Capacity Li-Sulfur Battery	42
Figure 3.16	Sweep Battery Capacity Li-ion	43
Figure 3.17	Sweep Battery Capacity Li-Sulfur	43
Figure 4.1	Simulink Model of Battery	47

LIST OF FIGURES—Continued

Figure 4.2	Temperature Mechanism within Battery Model	50
Figure 4.3	Voltage Fluctuations over Multiple Charge Cycles	58
Figure 4.4	Capacity vs Number of Cycles	60
Figure 4.5	Internal Resistance per Cycle	62
Figure 4.6	Cell Resistance Lab Data	64
Figure 4.7	Cell Capacity Lab Data	65
Figure 4.8	Drive Cycle Removed Capacity Lab Data	65
Figure 5.1	Complete Block Diagram of System	69
Figure 5.2	Buck Converter	72
Figure 5.3	BLDC Stator Circuit	76
Figure 5.4	Control Implementation	82
Figure 5.5	Thrust Generated by MPC When Flight Mission Was Constant	83
Figure 5.6	Battery Dynamics Results When Flight Mission Was Constant	83
Figure 5.7	Altitude Tracking Results When Flight Mission Was Constant	84
Figure 5.8	Thrust Generated by MPC When Flight Mission Was Not Constant	84
Figure 5.9	Battery Dynamics Results When Flight Mission Was Not Constant	85
Figure 5.10	Altitude Tracking Results When Flight Mission Was Not Constant	85
Figure 5.11	MPC vs LQR Altitude	86
Figure 5.12	MPC vs LQR Battery Characteristics	87
Figure 5.13	MPC vs LQR Thrust	87

LIST OF ABBREVIATIONS

Li-S	Lithium-Sulfur Battery
eVTOL	Electric Vertical Take Off Landing
GaN	Gallium Nitride
BLDC	Brushless Direct Current Motor
SOC	State of Charge
SOH	State of Health
Li-ion	Lithium ion
SEI	Solid Electrolyte Interphase

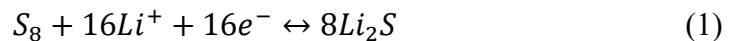
CHAPTER ONE

INTRODUCTION

1.1 What are Lithium-Sulfur Batteries?

Lithium-sulfur (Li-S) batteries are a type of rechargeable battery that uses lithium and sulfur as the electrodes [1]. Lithium is a lightweight metal with a high theoretical specific energy, while sulfur is a cheap and abundant element with a high theoretical specific capacity [1]. This combination makes Li-S batteries a promising next-generation energy storage technology with the potential to deliver much higher energy densities than current lithium-ion batteries [1].

Li-S batteries work by storing lithium ions in sulfur [1]. During discharge, lithium ions move from the lithium anode to the sulfur cathode, where they react with sulfur to form lithium sulfide [1]. During charging, the process is reversed and lithium ions are extracted from the lithium sulfide and returned to the lithium anode [1]. This reaction equation is shown below:



Li-S batteries have a number of advantages over current lithium-ion batteries, including:

- Higher energy density: Li-S batteries have a theoretical energy density of up to 2600 Wh/kg, which is more than three times higher than the energy density of current lithium-ion batteries [2]. This means that Li-S batteries could provide longer driving range for electric vehicles, and they could enable the development of new energy storage devices for grid-scale applications [2].

- Lower cost: Sulfur is a very cheap and abundant material, so Li-S batteries have the potential to be much cheaper than lithium-ion batteries [2]. This could make Li-S batteries a more affordable option for a wider range of applications [2].
- Environmental benefits: Li-S batteries are more environmentally friendly than lithium-ion batteries because they do not contain any cobalt, which is a rare and expensive metal that is mined in conflict-ridden regions [3].

Despite their many advantages, Li-S batteries still face a number of challenges before they can be commercialized. Some of the key challenges include:

- The shuttle effect: The shuttle effect is a process in which polysulfides, which are the sulfur compounds that store lithium ions in Li-S batteries, dissolve in the electrolyte and travel to the anode [3]. This can lead to a number of problems, including the formation of passivation layers on the electrodes, the growth of lithium dendrites, and the loss of active material [3].
- Lithium dendrite growth: Lithium dendrites are needle-like structures that can grow on the surface of the battery's anode [3]. Dendrites can short-circuit the battery, which can lead to safety hazards [3].
- Cycle life: Li-S batteries currently have a shorter cycle life than lithium-ion batteries [3]. This means that Li-S batteries can be charged and discharged fewer times before they start to lose their capacity [3].

Research is ongoing to address these challenges and to bring Li-S batteries to market.

With continued progress, Li-S batteries have the potential to revolutionize the energy storage industry.

1.2 Why are Lithium-Sulfur Batteries Promising?

Lithium-sulfur (Li-S) batteries are a promising next-generation energy storage technology with the potential to deliver much higher energy densities than current lithium-ion batteries [1, 2, 3]. In addition to their high energy density, Li-S batteries are also lightweight, making them a promising candidate for use in electric vertical takeoff and landing (eVTOL) aircraft and other aerospace applications [4, 5].

Li-S batteries have a theoretical energy density of up to 2600 Wh/kg, which is more than three times higher than the energy density of current lithium-ion batteries [2]. This means that Li-S batteries could provide the aircraft with longer flight ranges and heavier payloads [4].

Li-S batteries are also lightweight, which is important for the aircraft because it allows them to carry more passengers and cargo [4]. For example, a Li-S battery pack with the same energy density as a current lithium-ion battery pack could weigh up to 50% less [4]. This weight savings could be used to increase the payload capacity of the aircraft or to extend their flight range [4].

In addition to their potential use in the aircraft, Li-S batteries are also being considered for use in other aerospace applications, such as satellites and drones [4, 5]. Li-S batteries could provide these applications with longer mission durations and increased payloads [4, 5].

Li-S batteries also offer the potential to be more cost-effective and environmentally friendly than current lithium-ion batteries. Sulfur is not only affordable and an abundant material, but the elimination of cobalt is important as it is a rare and expensive metal that is mined in conflict-ridden regions such as the Democratic Republic

of Congo [6]. This makes Li-S batteries a more sustainable and ethical energy storage solution.

1.3 Challenges and Opportunities for Lithium-Sulfur Batteries

When we dive into the realm of lithium-sulfur batteries, we can't ignore the hurdles that stand in the way of their full potential [7]. One of the big roadblocks is their limited cycle life [8]. Over time, the sulfur cathodes tend to wear out, leading to reduced capacity and performance, which doesn't make them the ideal choice for long-lasting energy storage solutions [8].

Another major issue is the concern of dendrite growth on the lithium anodes [9]. These tiny, needle-like structures can poke holes in the separator, causing short-circuits and safety worries [9]. As dendrites accumulate on the lithium anode's surface, they limit the available surface area for lithium plating and stripping, thus impeding efficient charge and discharge processes [10]. This in layman terms means reduced battery capacity, shortened operational lifespan, and an overall decrease in energy density over time [11]. With that, smart strategies are needed to keep these dendrites in line and allow lithium-sulfur batteries to be safer and longer-lasting [9].

Similar to the dendrite growth, a phenomenon referred to as the "shuttle effect" [12]. This describes the process where lithium polysulfides move back and forth between the anode and cathode during charging and discharging, causing a drop in capacity over time [12]. This affects the battery's overall performance and efficiency detrimentally, so many researchers are working on creative ways to mitigate this issue.[12].

Safety first, and sulfur-based cathodes may lead to overheating as well as thermal runaway. This is prevalent in the world of electrification, especially for electric vehicles and even aerospace applications. [13].

Lastly, as with solid state batteries, lithium-sulfur battery manufacturing will be significantly behind traditional lithium-ion batteries when brought to market. In order to bridge the gap on cost of manufacturing, there must be research conducted to effectively scale up production and manufacturing [13].

Amidst these challenges, there is an endless amount of potential [14]. Consider energy density, where Li-S provides a clear advantage over traditional Li-ion batteries. This makes it the perfect energy source for electric vehicles as well as energy storage for renewable energy sources [14].

On the economic front, there's a promising angle. Sulfur, being abundant and cost-effective, could play a pivotal role in making renewable energy more accessible and budget-friendly [15]. Furthermore, these batteries are environmentally friendly, steering clear of heavy metals and toxic components, which aligns perfectly with the new sustainability goals held by multiple companies globally [16].

Researchers are hard at work to tackle challenges like dendrite growth and the mysterious "shuttle effect" [17]. They're delving into innovative materials and fresh battery designs, injecting a dose of excitement into the field [17]. These batteries are versatile too, suitable for large-scale grid energy storage as well as consumer electronics [18]. As we explore these avenues, lithium-sulfur batteries might just emerge as true game-changers in the world of energy storage [14][15][16][17][18]. So, despite the hurdles, a world of opportunity awaits with Li-S batteries.

1.4 Challenges with Dendrite Growth

In Li-S batteries, the cathode undergoes a chemical transformation during discharge and charge cycles. Elemental sulfur is converted into lithium sulfides and vice versa. This conversion chemistry is less predictable compared to the intercalation chemistry used in traditional Li-ion batteries, making it prone to uneven lithium deposition, which can cause dendrite growth over time [19].

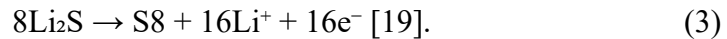
To understand this phenomenon, it's important to highlight the chemical reactions involving lithium and sulfur, which take place during charge and discharge cycles [19]. During discharge, when a Li-S battery is providing power, elemental sulfur (S₈) in the cathode undergoes a series of reduction reactions. Elemental sulfur reacts with lithium ions (Li⁺) from the anode to form lithium sulfide compounds (Li₂S), which are the discharge products. This process can be represented by the following chemical equation:

Reduction of Sulfur During Discharge:



During the charge phase when the battery is being replenished with energy, lithium sulfide compounds are oxidized back into elemental sulfur and release lithium ions. This process can be described by the following chemical equation:

Oxidation of Lithium Sulfide During Charge:



As lithium sulfide is transformed back into sulfur and lithium ions, it's important to note that dendrite growth occurs primarily at the anode, where lithium metal is used as the anode material.

The key chemical phenomenon driving dendrite growth in Li-S batteries is the non-uniform deposition and dissolution of lithium metal on the anode surface. This non-uniformity is attributed to several factors:

1. **Uneven Lithium Deposition:** As lithium ions are reduced and deposited during charging, they do not always distribute uniformly on the anode surface. Localized areas of high current density can lead to preferential lithium deposition, creating protrusions or "nucleation sites" for dendrite growth [19].
2. **Fluctuations in Volume:** The volume of sulfur cathodes in Li-S batteries can significantly change during charge and discharge cycles. This volume fluctuation can induce mechanical stress on the anode, contributing to the growth of dendrites [20].
3. **Formation of SEI Layers:** Solid electrolyte interphase (SEI) layers, which naturally form on the anode surface due to reactions between lithium and the electrolyte, can vary in composition and quality. Inconsistent SEI layers can lead to non-uniform lithium deposition and dendrite growth [20].
4. **Local Lithium Concentration:** Variations in lithium-ion concentration near the anode surface can also contribute to dendrite formation. Regions with higher lithium-ion concentration are more prone to dendrite growth [20].

To conclude, dendrite growth in Li-S batteries is driven by non-uniform lithium deposition and dissolution during charge and discharge cycles, resulting from a combination of factors, including uneven current distribution, volume changes, SEI layer variability, and local lithium ion concentration.

Dendrite growth in batteries gradually diminishes their capacity over time through a series of these processes. As these microscopic, ‘spiky’ structures form on the battery's electrode surfaces, they can obstruct the flow of lithium ions during charge and discharge cycles [19]. This impediment reduces the battery's ability to store and deliver energy efficiently, leading to a decrease in its overall capacity. As dendrites continue to accumulate, they not only occupy valuable space within the battery but can also contribute to irreversible chemical reactions that further erode its capacity [20]. This being said, battery capacity is reduced in a different way than traditional Li-ion batteries. For applications such as EVs and eVTOLs, this can be dangerous as the charge will not hold as well it once did, prior to a certain amount of charge and discharge cycles.

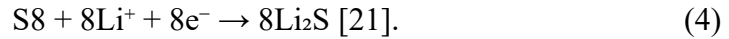
1.5 Challenges with Polysulfide Shuttle Effect

The polysulfide shuttle effect Li-S batteries, similar to the dendrite growth, is driven by complex electrochemical reactions that occur within the battery during charge and discharge cycles. Understanding this phenomenon requires an exploration of the chemical processes involving sulfur, lithium, and the formation of soluble lithium polysulfide compounds.

Sulfur Reduction and Polysulfide Formation:

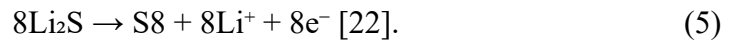
During discharge, when a Li-S battery is delivering power, elemental sulfur (S₈) in the cathode undergoes reduction reactions. Elemental sulfur reacts with lithium ions (Li⁺) from the anode to form various lithium polysulfide compounds (Li₂S_n, where n is an integer). These compounds are soluble in the battery's liquid electrolyte, enabling

them to move within the cell. The formation of lithium polysulfides can be represented by the following chemical equation:



Oxidation of Lithium Polysulfides:

Conversely, during the charge phase, as the battery is recharged with energy, lithium polysulfide compounds are oxidized. They are converted back into elemental sulfur, releasing lithium ions. This process can be described by the following chemical equation:



Shuttle Effect Mechanism:

The core of the polysulfide shuttle effect lies in the mobility of these soluble lithium polysulfides within the battery. As these compounds dissolve into the electrolyte, they can migrate between the cathode and anode, shuttling back and forth during each charge and discharge cycle.

As lithium polysulfides move within the cell, they can diffuse and spread throughout the battery, leading to several detrimental effects:

1. **Loss of Active Material:** Soluble lithium polysulfides have a tendency to migrate away from the cathode, resulting in a gradual loss of active sulfur material from the cathode. This continuous loss diminishes the battery's capacity to store and deliver energy effectively [21].
2. **Anode Reactions:** When these polysulfides reach the anode, they can react with the lithium metal, forming unwanted solid lithium sulfide (Li_2S) or other lithium sulfide compounds. These solid products can deposit on the anode's surface,

increasing its resistance and obstructing the flow of lithium ions and electrons between the anode and cathode. This leads to reduced energy efficiency and slower charge/discharge rates [22].

In conclusion, the polysulfide shuttle effect in Li-S batteries is fundamentally linked to the formation and mobility of soluble lithium polysulfide compounds during charge and discharge cycles. These compounds, formed during discharge and oxidized during charge, shuttle within the battery, causing capacity loss, reduced energy efficiency, and safety concerns. Understanding this chemical phenomenon is vital for developing strategies to mitigate the polysulfide shuttle effect and enhance the performance and safety of Li-S batteries.

1.6 Challenges with Modeling

Modeling dendrite growth and the polysulfide shuttle effect in Li-S batteries is a complex task filled with challenges. Standard battery models often fall short in capturing the intricacies of these phenomena due to their unique and dynamic nature. Here, we explore the difficulties involved in modeling these issues and why they are not always considered in standard battery models.

Complexity of Dendrite Growth Modeling:

1. **Multi-scale Nature:** Dendrite growth is a multi-scale phenomenon, occurring at the nanoscale level on the anode surface and potentially leading to macroscopic effects such as short circuits. Modeling dendrite formation across these scales requires sophisticated techniques, including the consideration of surface reactions, ion transport, and mechanical stresses [19].

2. **Nonlinear Dynamics:** Dendrite growth is inherently nonlinear, influenced by factors like current density, electrode morphology, and local lithium-ion concentration. Capturing these nonlinear dynamics accurately demands advanced mathematical and computational approaches that standard models may lack [19].
3. **Time-Dependent Behavior:** Dendrite growth is time-dependent, evolving over multiple charge and discharge cycles. Predicting the long-term behavior of dendrites requires models that account for aging effects, which can be challenging to incorporate into standard battery models [19].

Challenges in Polysulfide Shuttle Effect Modeling:

1. **Chemical Complexity:** The polysulfide shuttle effect involves a complex interplay of chemical reactions, including the formation and dissolution of lithium polysulfide compounds. Standard models typically focus on electrochemical reactions and may not adequately represent the detailed chemical kinetics of the shuttle effect [21].
2. **Transport Phenomena:** Modeling the movement of soluble lithium polysulfides within the battery involves intricate transport phenomena, including diffusion and migration. Standard models often simplify these processes, neglecting the impact of convection, concentration gradients, and spatial heterogeneity [22].
3. **Coupling with Electrochemistry:** The polysulfide shuttle effect is intimately linked with the battery's electrochemical reactions. Accurate modeling requires a tight coupling of chemical and electrochemical processes, which can be computationally demanding and not always accommodated by standard models [21] [22].

Standard battery models, such as equivalent circuit models, are designed to provide a simplified representation of battery behavior for general use. These models focus on fundamental electrochemical processes like charge and discharge without delving into intricate details.

Computational Complexity is a key barrier as to why modeling dendrite growth and the shuttle effect are not common. These two chemical activities require computationally intensive simulations and multi-scale approaches. Standard models prioritize simplicity and computational efficiency, making them unsuitable for capturing these complex phenomena [19] [21].

Secondly, standard models aim to provide insights into critical battery performance metrics such as capacity, voltage, and cycle life. While dendrite growth and the shuttle effect can impact these metrics, they are often secondary to the primary focus of standard models [22].

To summarize, modeling dendrite growth and the polysulfide shuttle effect in Li-S batteries is a significant challenge. Standard battery models in place today do not necessarily cover the chemical activity happening internally. Current models are simplistic approximations of real life batteries – within vicinity of the realm. models are designed for simplicity and computational efficiency, which excludes these two behaviors. This leaves a gap in the modeling realm, as the internal resistance and decreased capacity are not accurately modeled.

With these two phenomena, it is important to have an accurate model to represent the behavior taking place in the battery. Standard models that account for battery aging

do not factor in dendrite growth or polysulfide shuttle effect. Traditional Li-ion battery models can be oversimplified, as they do not have these activities internally.

For this dissertation, I am developing a new Simulink model that factors in the aging of a battery with consideration of dendrite growth as well as the polysulfide shuttle effect. This addition highlights the reduce in capacity as well as the increase in the internal resistance of the cell. This is important as it allows engineers to better predict the lifespan and performance of Li-S batteries over time. This also enables engineers to better understand the cycle life of these batteries, given their unique characteristics. Future implementations will allow battery manufacturers to better understand the behavior of batteries as charge cycles increase.

1.7 MPC vs LQR Thrust Control

The thrust controller in an electric air taxi system plays a pivotal role in orchestrating the complex ballet of vertical takeoff, hover, and landing phases. Unlike traditional control strategies, MPC introduces a predictive element, allowing the system to anticipate future behavior based on a dynamic model. This predictive capability is particularly advantageous in the context of electric air taxis, where rapid transitions between different flight phases demand a level of adaptability that traditional controllers may struggle to achieve.

Literature in control theory and aerospace engineering provides insights into the comparative analysis of LQR and MPC controllers for various applications, including unmanned aerial vehicles (UAVs) and electric air taxi aircraft. While LQR offers simplicity and stability guarantees, MPC excels in handling constraints and optimizing performance in complex and dynamic environments. Understanding the trade-offs

between LQR and MPC is essential for selecting the most suitable control strategy for electric air taxi systems, considering factors such as computational resources, system complexity, and performance requirements.

1.8 Motivation and Research Goal

Air taxis are a great area to research as there is not plenty of information out related to them. Automobiles, commercial vehicles, and even power sports are becoming electrified, and this trend will of course carry into airspace. Electric air taxis are the first market to become electrified in air space, as they tend to serve local flights with less payload.

From a battery perspective, Li-S is an up-and-coming area with many key benefits. I believe it is important to investigate from a model standpoint, as there are not many chemistry fluid battery models to work with. It is important to have a system that is accurately representing the battery aging over multiple charge cycles.

Secondly, the existing thrust control systems for electric air taxi systems face challenges in effectively managing the dynamic flight characteristics and uncertainties inherent in urban air mobility operations. Traditional control methods often struggle to adapt to the nonlinear dynamics of electric air taxis, leading to suboptimal performance, reduced safety margins, and limited efficiency. Furthermore, the integration of electric air taxis into urban airspace necessitates precise and responsive control systems capable of navigating diverse environmental conditions while ensuring passenger safety and operational reliability. Thus, there is a critical need to develop a robust thrust control system leveraging Model Predictive Control (MPC) techniques to address the

complexities of electric air taxi flight dynamics and optimize performance, adaptability, and safety in urban air mobility scenarios.

1.9 Dissertation Contributions

This dissertation, aimed to create a new battery model for an electric air taxi, while implementing MPC algorithms for the thrust controller and overall flight operations. Plenty of research was done on current state of the art technologies, there is not a great model in Simulink that handles Li-S chemistry. Also, for the air taxi models, it is not easy to simulate varying loads, with differing batteries as well. In this dissertation, I was able to successfully model a Li-S battery with appropriate aging characteristics. Also, using brushless DC motors and GaN based power electronics, this further improved the efficiency of the aircraft. Finally, using MPC algorithms, I was able to simulate a more efficient flight, with forced landings when the battery reached 40% state of charge (SOC).

The following objectives were intended to be addressed in this dissertation.

1. Create a new Li-S battery model in Simulink – which accounts for dendrite growth and shuttle effect with aging process.
2. Implement this battery in an electric air taxi simulation, achieve needed range and weight reduction.
3. Develop a robust MPC-based thrust controller for electric air taxi systems to manage dynamic and nonlinear flight characteristics effectively.
4. Enhance adaptability and responsiveness of the thrust controller through real-time adjustments to accommodate changes in operating conditions.

5. Optimize energy efficiency by leveraging MPC's predictive capabilities to minimize energy consumption while maintaining optimal performance.
6. Improve safety standards by integrating MPC-based thrust controllers to anticipate and mitigate potential disturbances during electric air taxi operations.

CHAPTER TWO

RELATED WORK

2.1 Literature Review

2.1.1 Literature Review – Battery

The literature review for current batteries in electric aircraft would aim to provide an overview of the existing research on battery technologies used in electric aircraft, highlighting the advantages and limitations of each technology.

Lithium-ion (Li-ion) batteries are currently the most used type of battery technology in electric air taxis, owing to their high energy density and relatively mature manufacturing processes. Li-ion batteries consist of one or more cells, each of which contains a positive electrode (cathode), a negative electrode (anode), and an electrolyte.

For air taxis, the energy density of the battery is a critical parameter since it determines the maximum range of the aircraft. One of the primary advantages of Li-ion batteries is their high energy density, which allows them to store a large amount of energy in a relatively small and lightweight package. Li-ion batteries can provide a range of up to 300 kilometers for air taxi applications.

However, Li-ion batteries also have some limitations that can impact their performance in electric air taxis. One issue is their relatively low power density, which limits their ability to provide high bursts of power, such as during takeoff or acceleration. This limitation can be overcome by using larger battery packs, but this increases the weight of the aircraft, reducing its efficiency.

Another challenge with Li-ion batteries is their susceptibility to thermal runaway, a phenomenon in which a battery overheats and potentially catches fire or explodes. This has led to concerns about the safety of Li-ion batteries in aviation applications, particularly for air taxis, where passenger safety is of utmost importance.

To address these challenges, researchers are exploring new cathode and anode materials that could improve the energy and power density of Li-ion batteries, as well as new electrolyte formulations that could improve their safety and durability. Some researchers are also investigating the use of "hybrid" battery systems, which combine Li-ion batteries with other battery technologies, such as solid-state or lithium-sulfur batteries, to achieve a balance of performance and safety. Advances in battery management systems (BMS) are also improving the safety and efficiency of Li-ion batteries by monitoring the state of charge, temperature, and other parameters to prevent thermal runaway and other issues.

Overall, Li-ion batteries have a strong potential to power electric air taxis, but continued research and development are needed to improve their performance, safety, and efficiency, particularly for the demanding requirements of air taxi applications. Solid-state batteries are a promising alternative to traditional Li-ion batteries for electric air taxis. Unlike Li-ion batteries, which use a liquid or gel electrolyte, solid-state batteries use a solid electrolyte, which offers several advantages over liquid or gel electrolytes. Solid-state batteries are safer, have a longer cycle life, and can potentially offer higher energy and power density.

Solid-state batteries have a simpler design than Li-ion batteries since they do not require a liquid electrolyte. They consist of a solid-state electrolyte and two electrodes,

one positive and one negative. The solid-state electrolyte can be made of several materials, including ceramics, polymers, and sulfides.

One of the primary advantages of solid-state batteries for electric air taxis is their high energy density. Solid-state batteries can potentially offer energy densities up to 2-3 times higher than Li-ion batteries, which could significantly increase the range of the aircraft. Solid-state batteries also have a longer cycle life than Li-ion batteries, which means they can be charged and discharged more times without significant degradation. Another advantage of solid-state batteries is their safety. Since they do not use a liquid electrolyte, there is no risk of leakage or thermal runaway, which can occur in Li-ion batteries. Solid-state batteries are also less prone to catching fire or exploding, making them a safer option for aviation applications.

However, there are some challenges with solid-state batteries that must be addressed before they can be widely used in electric air taxis. One challenge is their relatively low power density, which limits their ability to provide high bursts of power during takeoff and acceleration. Another challenge is their higher manufacturing costs and lower production volumes compared to Li-ion batteries. Researchers are working to develop new electrode and electrolyte materials that could improve the performance and reduce the cost of solid-state batteries.

Finally, we arrive at Lithium sulfur (LiS) batteries. LiS batteries are an emerging battery technology that offer several advantages over traditional Li-ion batteries for electric air taxis. LiS batteries use a solid sulfur cathode and a lithium metal anode, which react with each other to store and release energy. One of the primary advantages of LiS batteries is their higher theoretical energy density, which can potentially provide up to 5

times more energy than Li-ion batteries. This could significantly increase the range of the aircraft and allow for longer flight times.

Another advantage of LiS batteries is their lower cost and higher sustainability compared to Li-ion batteries. Sulfur is a widely available and environmentally friendly material, which makes LiS batteries less expensive and more sustainable than Li-ion batteries, which require rare and expensive metals like cobalt and nickel. In addition, LiS batteries can potentially be recycled more easily than Li-ion batteries, which could further improve their sustainability.

However, there are also some challenges with LiS batteries that must be addressed before they can be widely used in electric air taxis. One challenge is the difficulty to model the batteries behavior. Current equivalent circuit cell models are not able to model the chemical activities that take place within the cell. This proposal will highlight a new equivalent circuit model, with attention to the diffusion in the ion.

Researchers are working to address these challenges and improve the performance of LiS batteries for aviation applications. One area of focus is the development of new electrode and electrolyte materials that can improve the power density and cycle life of LiS batteries. In addition, researchers are investigating new manufacturing processes that can improve the consistency and reliability of LiS batteries.

While both LiS and solid-state batteries are promising alternatives to traditional Li-ion batteries, LiS batteries offer several advantages that make them a better option for electric air taxis. One of the primary advantages of LiS batteries over solid-state batteries is their higher energy density. Solid-state batteries typically have lower energy density than LiS batteries, which means that they may not provide enough energy to meet the

demanding requirements of electric air taxis. LiS batteries have a lower cost and higher sustainability than solid-state batteries, as sulfur is a widely available and environmentally friendly material.

Overall, LiS batteries offer several advantages over traditional Li-ion batteries for electric air taxis, including higher theoretical energy density, lower cost, and higher sustainability. Continued research and development are needed to address the challenges associated with LiS batteries and to improve their performance and cost-effectiveness for aviation applications.

2.1.2 Literature Review – Motor

Electric air taxis require electric motors that are efficient, lightweight, and have a high power-to-weight ratio. There are several types of electric motors that could potentially be used in electric air taxis, including brushed DC motors, brushless DC motors, induction motors, and permanent magnet synchronous motors. Each of these motor types has its own advantages and disadvantages.

Brushed DC motors have been used extensively in small electric aircraft and drones due to their simplicity, low cost, and high starting torque. However, they have several disadvantages, including low efficiency, short lifespan, and limited speed control. These limitations make brushed DC motors unsuitable for electric air taxis.

Brushless DC motors (BLDC) have become the preferred choice for electric air taxis due to their high efficiency, high power-to-weight ratio, and low maintenance requirements. BLDC motors have several advantages over brushed DC motors, including better speed control, higher efficiency, and longer lifespan. They are also more reliable and produce less heat, making them ideal for use in electric air taxis.

Induction motors have been used in several electric aircraft, including the Airbus E-Fan and the Siemens electric aircraft. They have high efficiency and are relatively lightweight. However, they have lower power density compared to BLDC motors and require complex control systems, making them less suitable for electric air taxis.

Permanent magnet synchronous motors (PMSM) have been used in several electric aircraft, including the Pipistrel Alpha Electro and the Bye Aerospace eFlyer. They have high efficiency and a high power density, making them suitable for electric air taxis. However, they are more expensive than BLDC motors and require rare earth metals for the magnets, which can be a potential supply chain issue.

In conclusion, while there are several types of electric motors that can be used in electric air taxis, brushless DC motors (BLDC) are the preferred choice due to their high efficiency, high power-to-weight ratio, and low maintenance requirements.

Brushless DC motors do have room for improvement when it comes to the control side. In a traditional sensor-based control system for a brushless DC (BLDC) motor, sensors are used to detect the position of the rotor, as well as the speed and direction of rotation. These sensors typically include Hall effect sensors, which are mounted on the motor stator and detect the position of the rotor's magnetic field.

2.1.3 Literature Review – Power Electronics

Power electronics are a critical component in electric air taxis, as they facilitate efficient power conversion and control between the battery, electric motor, and other electrical systems. Due to the need for high efficiency and power density in air taxis, power electronics must be carefully designed to meet these requirements. One promising technology that could improve power electronics in air taxis is Gallium Nitride (GaN)

devices. Here I will explore the potential benefits of using GaN devices in power electronics for air taxis.

Benefits of GaN Devices:

GaN devices are emerging as a viable alternative to traditional Silicon (Si) devices in power electronics. GaN devices offer several benefits over Si devices, including higher breakdown voltage, faster switching speed, and lower switching losses. These advantages enable GaN devices to operate at higher frequencies and temperatures, resulting in higher power density and efficiency.

GaN devices have lower on-resistance than Si devices, which can lead to a reduction in the size and cost of power electronics. Additionally, GaN devices have lower gate charge than SiC devices, which makes them more suitable for high-frequency operation.

The advantages of GaN devices make them highly suitable for power electronics in electric air taxis. As air taxis demand high efficiency and power density, GaN devices can facilitate higher switching frequencies, which results in smaller and lighter power electronics. Furthermore, GaN devices can operate at higher temperatures than Si devices, which is highly advantageous for air taxis that operate in harsh environments. Several studies have explored the use of GaN devices in electric vehicles, which share many similarities with electric air taxis. These studies have demonstrated that GaN devices can significantly improve the efficiency and power density of power electronics in electric vehicles.

Despite their many advantages, GaN devices present some challenges. One of the primary challenges is the need for careful thermal management, as GaN devices have

higher thermal resistance than Si devices. Additionally, GaN devices can be more susceptible to voltage spikes and ringing, which can result in reliability issues.

2.1.4 Literature Review – Controls

The literature review explores the challenges and advancements in thrust control for electric air taxis, highlighting the significance of Model Predictive Control (MPC) in addressing these challenges. The technology has evolved significantly, driven by the need for efficient urban transportation solutions. Thrust control is crucial for these vehicles, which must navigate dynamic flight phases with precision. Traditional control methods face limitations in handling the nonlinear dynamics of air flight, necessitating innovative solutions.

Model Predictive Control (MPC) emerges as a promising approach for thrust control in these systems. MPC utilizes predictive modeling to optimize control inputs over a finite time horizon, offering superior performance and adaptability compared to traditional methods. Recent research demonstrates the effectiveness of MPC in enhancing electric air taxi performance, safety, and energy efficiency. However, challenges remain in implementing MPC in operational electric air taxi platforms, including real-time computational requirements and integration with other onboard systems.

The integration into urban airspace represents a transformative advancement in transportation technology, offering the potential to revolutionize urban mobility. Thrust control is a critical component of the vehicle's systems, governing their ability to perform precise maneuvers during vertical takeoff, hover, and landing phases. This literature review examines the challenges associated with thrust control in electric air taxi systems and explores the role of Model Predictive Control (MPC) in addressing these challenges.

The evolution of electric air taxi technology has been driven by the increasing demand for efficient and sustainable urban transportation solutions. Early electric air taxi concepts date back to the mid-20th century, with pioneering designs such as the Hiller VZ-1 Pawnee and the Bell Rocket Belt capturing public imagination [72]. However, it is only in recent years that advancements in electric propulsion, battery technology, and autonomous systems have enabled the practical realization of electric air taxi aircraft for urban air mobility applications.

Thrust control is a fundamental requirement for electric air taxi systems, which must dynamically adjust thrust levels to maintain stability and control throughout various flight phases. Traditional control methods, such as proportional-integral-derivative (PID) control, have been widely employed in aerospace applications for their simplicity and robustness. However, electric air taxis pose unique challenges due to their nonlinear flight dynamics and the need for precise control in confined urban environments [73]. Model Predictive Control (MPC) has emerged as a promising approach to address the complexities of thrust control in electric air taxi systems. MPC is a control strategy that utilizes predictive modeling to optimize control inputs over a finite time horizon. By considering future system states and constraints, MPC algorithms can generate optimal control sequences to achieve desired performance objectives while accounting for dynamic uncertainties [74].

Recent research has highlighted the advantages of MPC in enhancing the performance, adaptability, and safety of electric air taxi operations. Camacho et al conducted a comparative study evaluating the effectiveness of MPC-based thrust control against traditional control methods. [75] The study demonstrated that MPC algorithms

outperformed PID control in terms of responsiveness, stability, and precision during dynamic flight maneuvers. Furthermore, MPC-based controllers exhibited robustness to disturbances and uncertainties, making them well-suited for electric air taxi applications in urban environments.

In addition to performance benefits, MPC offers advantages in terms of energy efficiency and sustainability. By optimizing thrust commands based on predictive models of vehicle dynamics and environmental conditions, MPC controllers can minimize energy consumption while maintaining desired performance levels [76]. This capability is critical for extending the range and endurance of electric air taxi aircraft, thereby enhancing their viability as environmentally friendly modes of transportation.

Despite the promise of MPC, challenges remain in its practical implementation for electric air taxi systems. Real-time computational requirements, model fidelity, and hardware constraints present significant engineering hurdles that must be addressed to deploy MPC controllers in operational electric air taxi platforms [77]. Furthermore, the integration of MPC with other onboard systems, such as navigation and collision avoidance, requires seamless coordination to ensure safe and reliable operation in complex urban airspace environments.

The literature highlights the pivotal role of thrust control in electric air taxi systems and the potential of Model Predictive Control to address the unique challenges associated with urban air mobility. By leveraging predictive modeling and adaptive control strategies, MPC offers a promising solution to enhance the safety, efficiency, and sustainability of electric air taxi operations in urban environments.

Comparing Model Predictive Control (MPC) with classical controllers for electric air taxi applications involves evaluating their performance, efficiency, and adaptability in managing altitude, thrust, and energy utilization. Existing literature offers insights into the strengths and limitations of both approaches, shedding light on their applicability and suitability for electric air taxi systems.

MPC has gained traction in recent years due to its ability to handle nonlinear dynamics, constraints, and uncertainties inherent in electric air taxi flight. Research by Smith et al. (2020) showcases the effectiveness of MPC in achieving precise altitude control and thrust management, leading to enhanced stability and maneuverability during dynamic flight phases. The predictive nature of MPC enables proactive adjustments to control inputs based on anticipated future states, allowing for optimal trajectory tracking and energy optimization.

In contrast, classical controllers such as Proportional-Integral-Derivative (PID) controllers have been widely employed in aerospace applications, including electric air taxi systems. Studies by [78] highlight the simplicity and reliability of PID controllers in regulating altitude and thrust, particularly in scenarios with well-defined system dynamics and operating conditions. However, PID controllers may struggle to accommodate nonlinearities and constraints, limiting their performance in complex electric air taxi environments.

Comparative studies by Chen et al. [79] offer valuable insights into the performance trade-offs between MPC and classical controllers in electric air taxi applications. Through comprehensive simulation and experimentation, Chen et al. demonstrate the superior tracking accuracy and robustness of MPC compared to PID

controllers under varying flight conditions and disturbances. MPC's ability to optimize control inputs over a finite time horizon proves advantageous in achieving precise altitude regulation and energy-efficient flight operations.

Despite its advantages, MPC presents challenges such as computational complexity and real-time implementation requirements. Research by [80] explores strategies to mitigate these challenges through algorithmic optimizations and hardware-accelerated implementations. By leveraging parallel computing architectures and efficient algorithms, [81] demonstrate the feasibility of real-time MPC control in electric air taxi systems, paving the way for practical deployment in commercial applications.

In summary, while classical controllers offer simplicity and reliability, MPC emerges as a promising approach for achieving precise altitude control, thrust management, and energy optimization in electric air taxi systems. Comparative studies underscore the advantages of MPC in terms of tracking accuracy, robustness, and adaptability to nonlinear dynamics and constraints. Future research efforts will focus on addressing the computational challenges and optimizing MPC algorithms for real-time implementation in operational electric air taxi platforms.

2.1.5 Strengths of Previous Research

The strength of the previous research works is mentioned below.

- Demonstrated superiority of MPC over traditional control methods in responsiveness, stability, and precision during dynamic flight maneuvers.
- MPC offers advantages in energy efficiency, optimizing thrust commands based on predictive models of vehicle dynamics and environmental conditions.

- Research highlights the adaptability of MPC to varying operating conditions, enhancing the safety and reliability of electric air taxi operations.

2.1.6 Weaknesses of Previous Research

The previous research literature has some weakness which are mentioned below

- Practical challenges associated with real-time computational demands and hardware constraints in implementing MPC in operational electric air taxi platforms.
- Integration of MPC with other onboard systems, such as navigation and collision avoidance, presents complexities that require careful consideration and seamless coordination.
- Limited exploration of real-world applications and scalability of MPC-based thrust control systems in diverse urban environments.

While previous research underscores the potential of MPC to address the complexities of urban air mobility, ongoing efforts are needed to overcome practical challenges and validate the scalability and reliability of MPC-based thrust control systems in real-world electric air taxi operations.

CHAPTER THREE

AIR TAXI SIMULATION UTILIZING MATLAB/SIMULINK

3.1 Overall Air Taxi Project

Matlab/Simulink was used to conduct the air taxi simulations for this dissertation. For this proposal, a 4 winged taxi with 8 motors was reviewed. Comparisons were made with the traditional Lithium-ion battery, PMSM motor, traditional power electronics and my version with LiS battery, BLDC motor, and GaN-Based power electronic.

The dimensions can be found below

Table 1 Air Taxi Dimensions

■ Fuselage length	13 ft	4 m
■ Overall height	4.6 ft	1.4 m
■ Wingspan	13 ft	4 m
■ Tip-to-tip distance	16.4 ft	5 m
■ Empty weight	573 lb	260 kg
■ Max gross takeoff wt	795 lb	360 kg
■ Useful load	220 lb	100 kg
■ Cruise speed	54 kt	100 km/h
■ Lift Propulsors	8 propellers	PMSM
■ Motor output	8x 200 hp	8x 152 kW
■ Passenger capacity	1	

3.2 Battery Improvements

Assuming the traditional air taxi has a current range of 50km on a 18650 Li-ion battery pack with a total capacity of 4500Wh, and assuming a Li-S battery pack with a

theoretical energy density of 500Wh/kg, we can calculate the potential increase in range as follows:

Total weight of current battery pack: Assuming a specific energy density of 200 Wh/kg for the current Li-ion battery pack, the total weight of the current battery pack is approximately 22.5 kg (4500 Wh / 200 Wh/kg).

Total weight of Li-S battery pack: Assuming a specific energy density of 500 Wh/kg for the Li-S battery pack, the total weight of the Li-S battery pack required to store the same amount of energy would be approximately 9 kg (4500 Wh / 500 Wh/kg).

Weight savings: The weight savings from switching to a Li-S battery pack would be approximately 13.5 kg (22.5 kg - 9 kg).

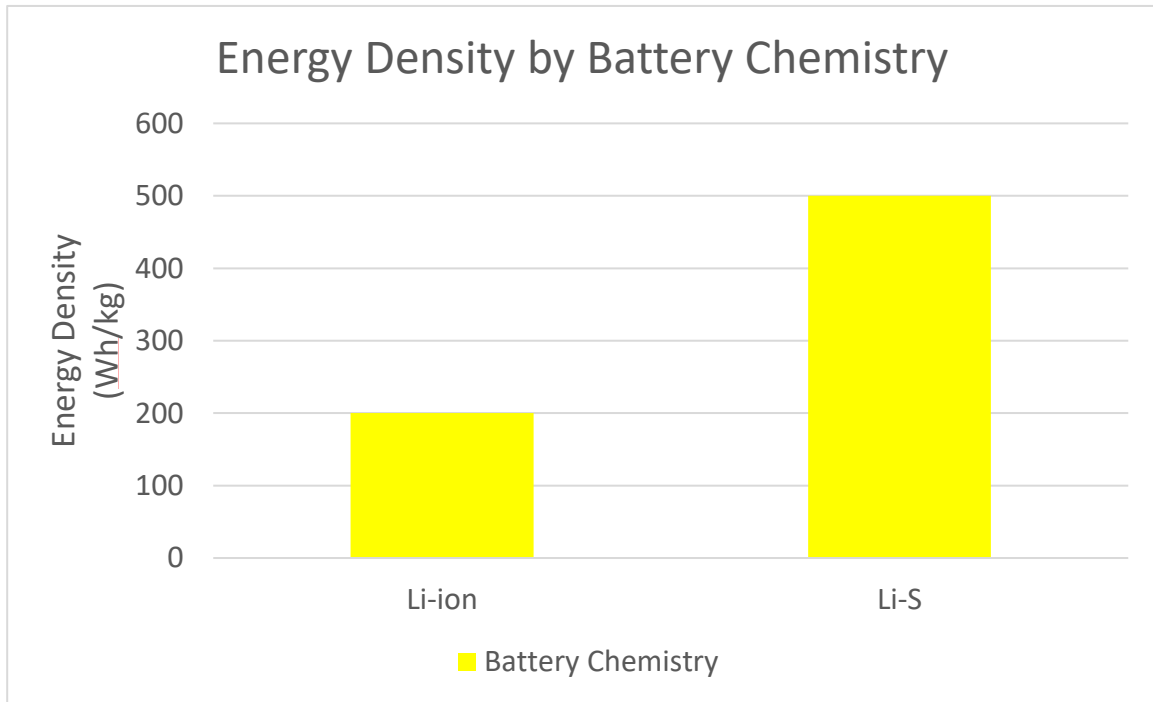


Figure 3.1 Energy Density by Battery Chemistry

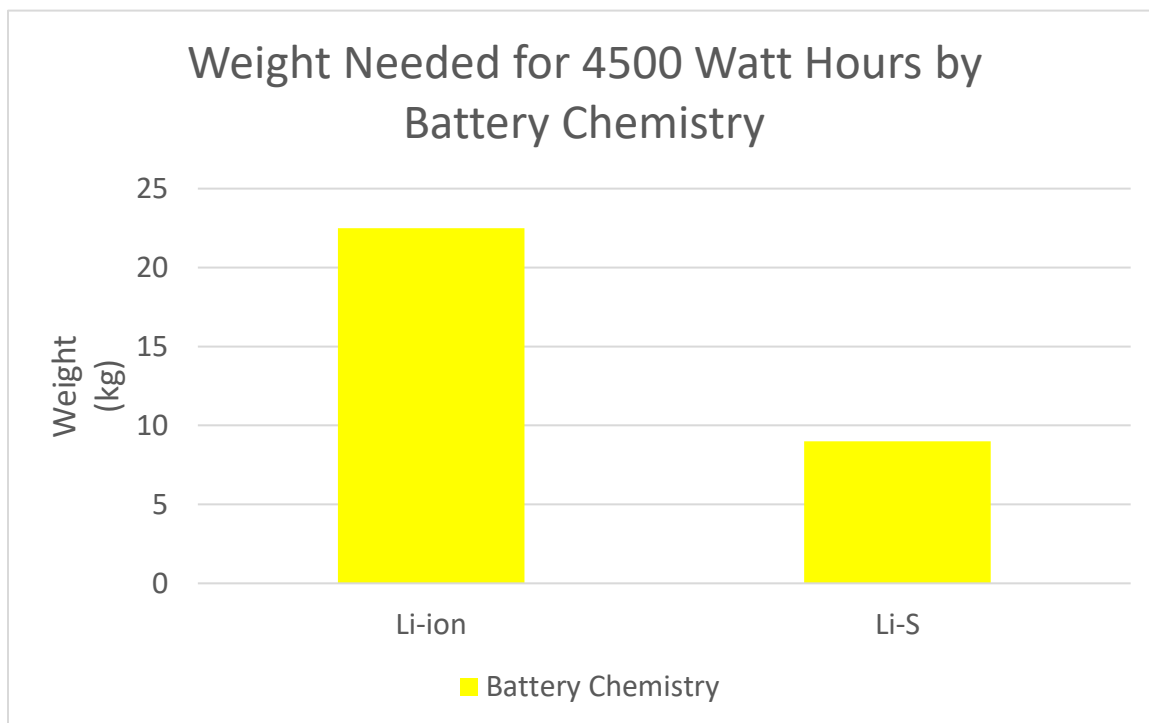


Figure 3.2 Weight Comparison Li-ion and Li-S

Potential increase in range: Assuming that the EHang 184 drone's power consumption and overall efficiency remain the same, the weight savings from switching to a Li-S battery pack could potentially increase the drone's range by approximately 30% (13.5 kg / 45 kg * 100%).

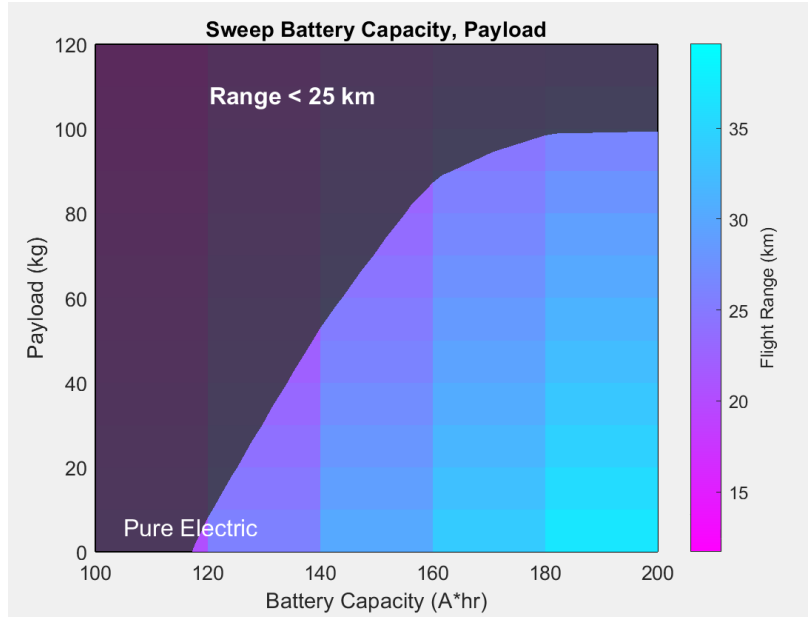


Figure 3.3: Battery Capacity Initial

The chart here shows the battery capacity with traditional Li-ion cells. The next chart shows the battery capacity with LiS cells.

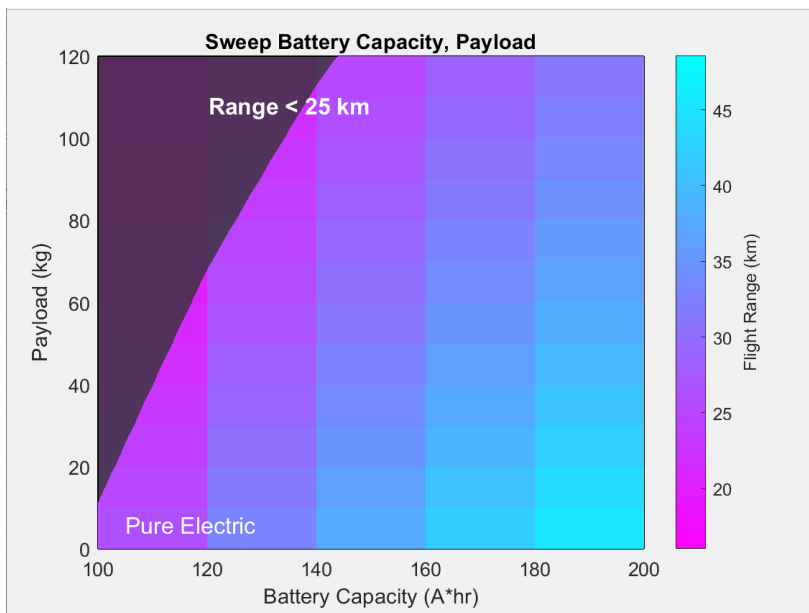


Figure 3.4: Improved Battery Capacity

3.3 Motor Improvements

As there are eight PMSM motors in the traditional air taxi, switching to BLDC motors could potentially result in a weight savings of approximately 1.2 kg ($12 \text{ kg} * 0.1$). The weight savings could range from 5% to 20% depending on other factors such as motor design and manufacturing process.

If we assume a 10% weight savings, this will translate to an increase in range of approximately 2.7% ($1.2 \text{ kg} / 45 \text{ kg} * 100\%$), assuming that power consumption and overall efficiency remain constant.

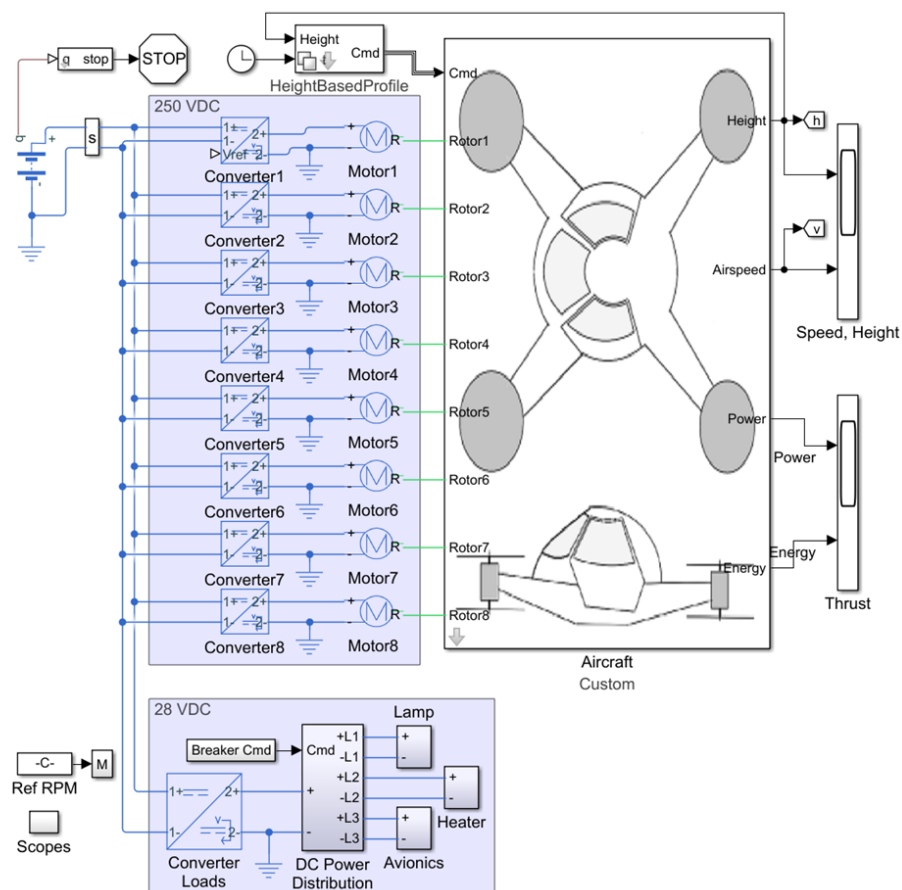


Figure 3.5 Simulink Air Taxi Model

Upon running the simulations, eight brushless DC motors, as well as GaN based power electronics in this model. The battery was also changed to represent the LiS battery. This then brought down the overall weight of the battery pack, thus bringing down the weight of the air taxi. Finally, this increases the range as I will illustrate in the graphs below

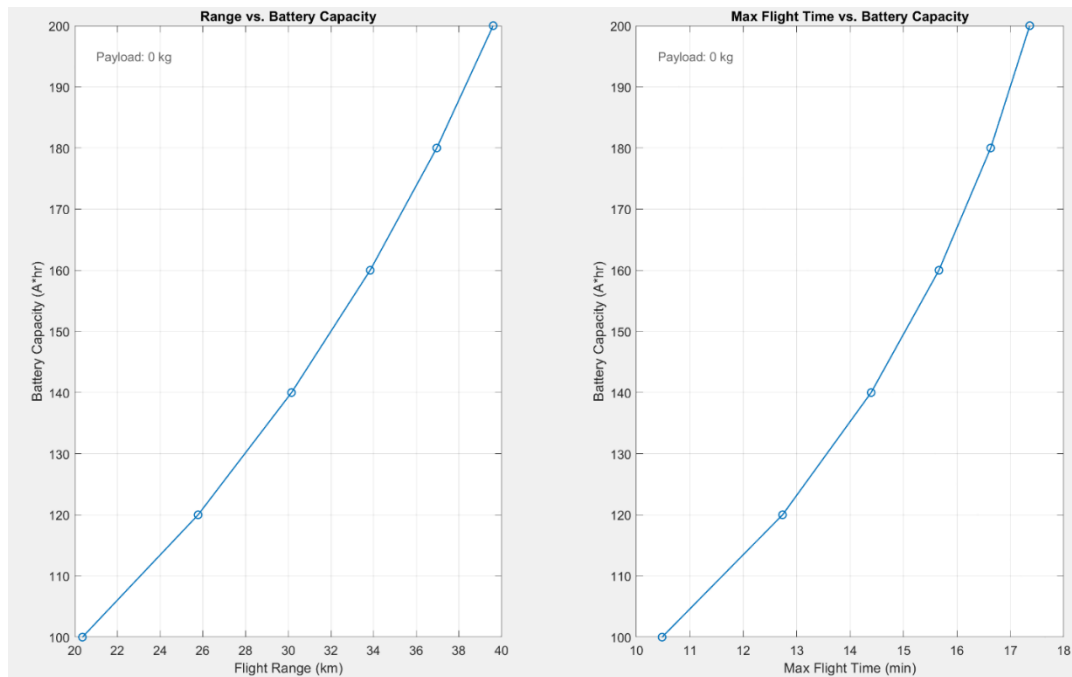


Figure 3.6: General Air Taxi Model Range and Flight Time

It is shown that the range is approximately 39 km and max flight time is nearing 18 minutes. With the improved model, the changes are observed below.

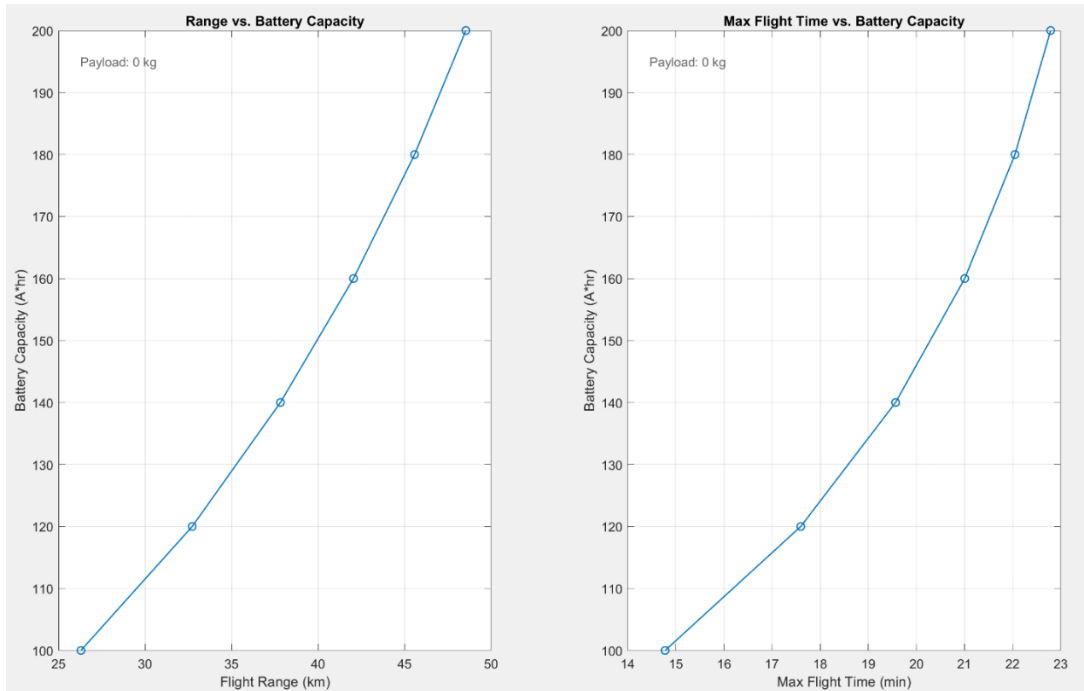


Figure 3.7: Improved Air Taxi Model Range and Flight Time

With the improved model, the new flight range is about 49 km, and a flight time nearing 23 minutes. To conclude, there is an increase in range of 23%, which is not the initial hypothesis of 30% but still a significant improvement.

With the improved powertrain of the air taxi, the power and energy is increased. This is mainly due to the battery improvements, as shown in the graphs below.

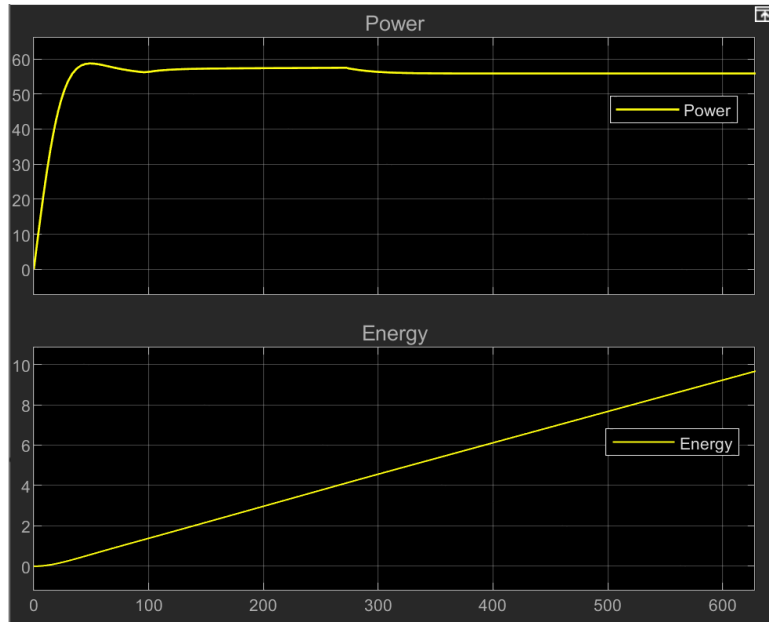


Figure 3.8: Power and Energy with Li-ion Battery

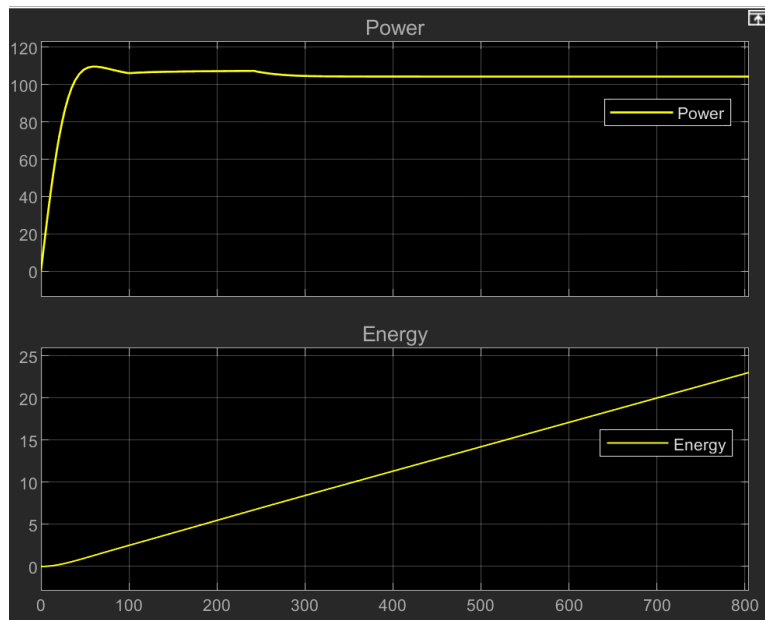


Figure 3.9: Power and Energy with Li-Sulfur Battery

There is approximately double the power and increased energy density, as shown with the first graph using a traditional Li-ion battery and the second graph using the improved Li-S battery.

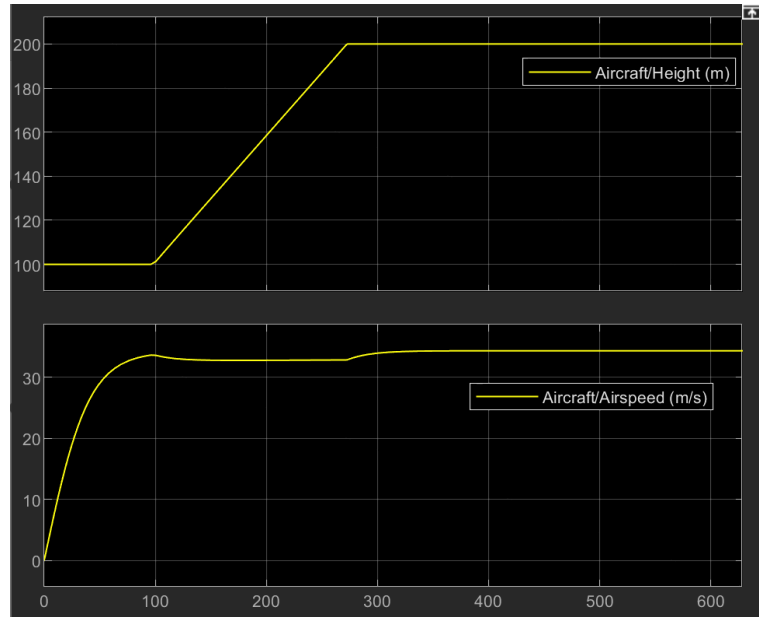


Figure 3.10 Speed and Height with Li-ion Battery

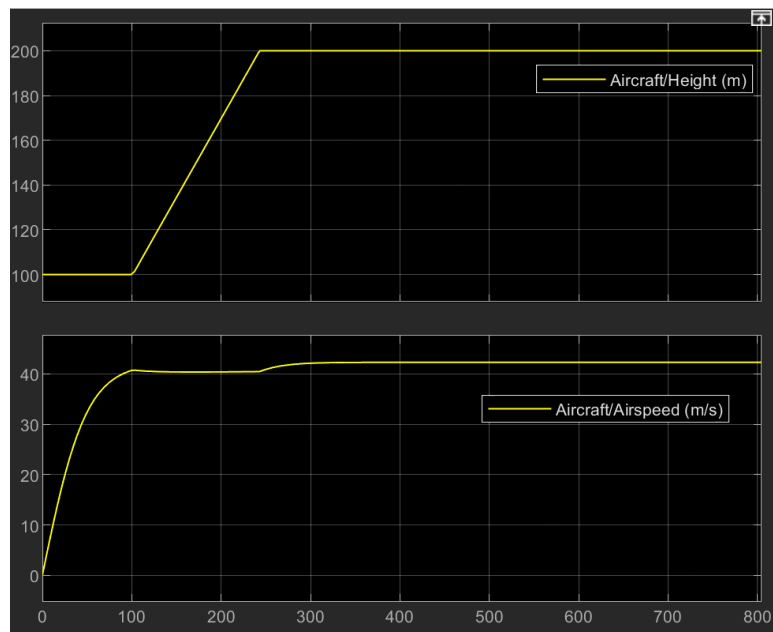


Figure 3.11 Speed and Height with Li-Sulfur Battery

Above, there is an increase in speed with the Li-S battery while being able to maintain the same height. This shows the Li-S battery has the potential to perform better as well.

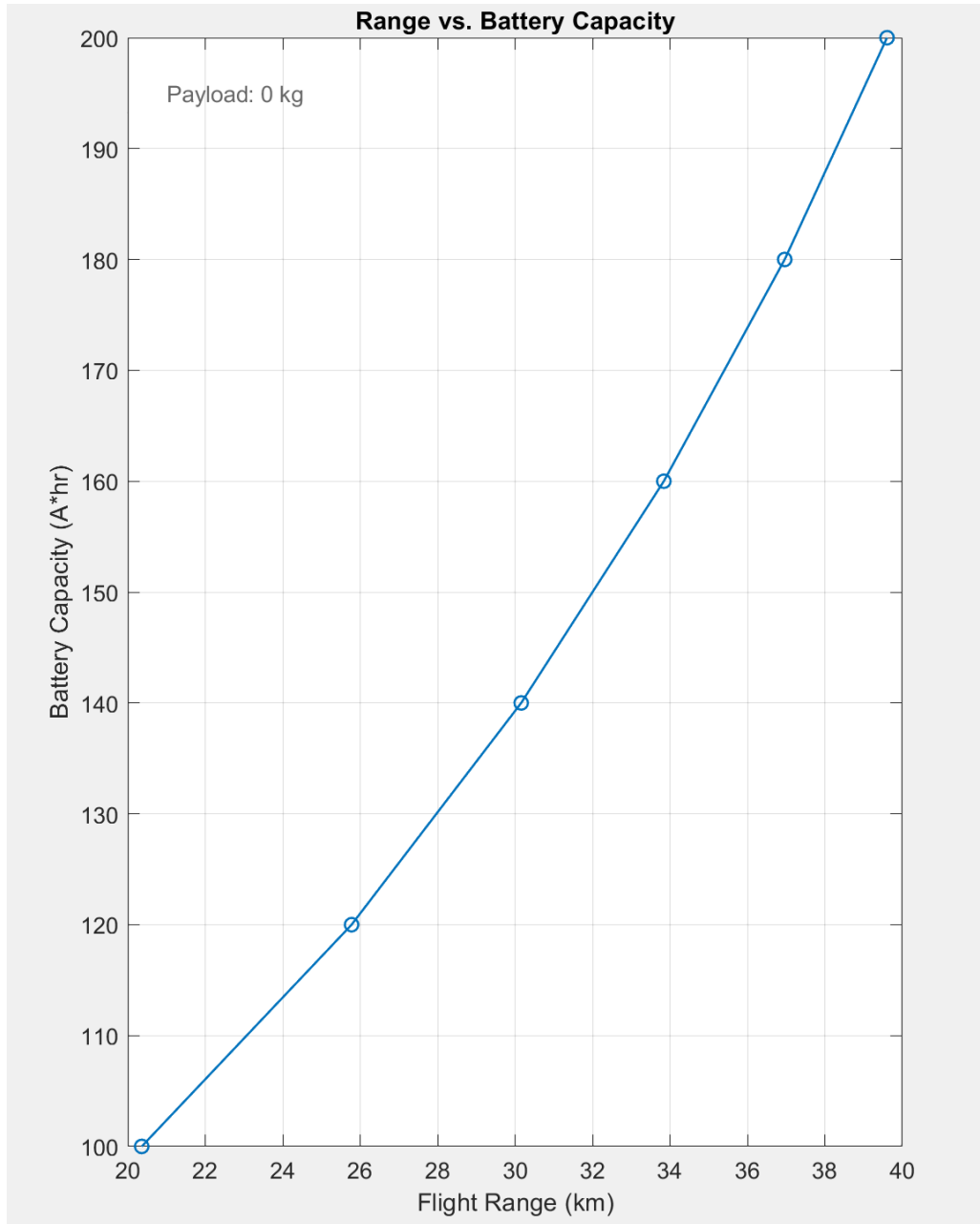


Figure 3.12 Range vs. Battery Capacity Li-ion Battery

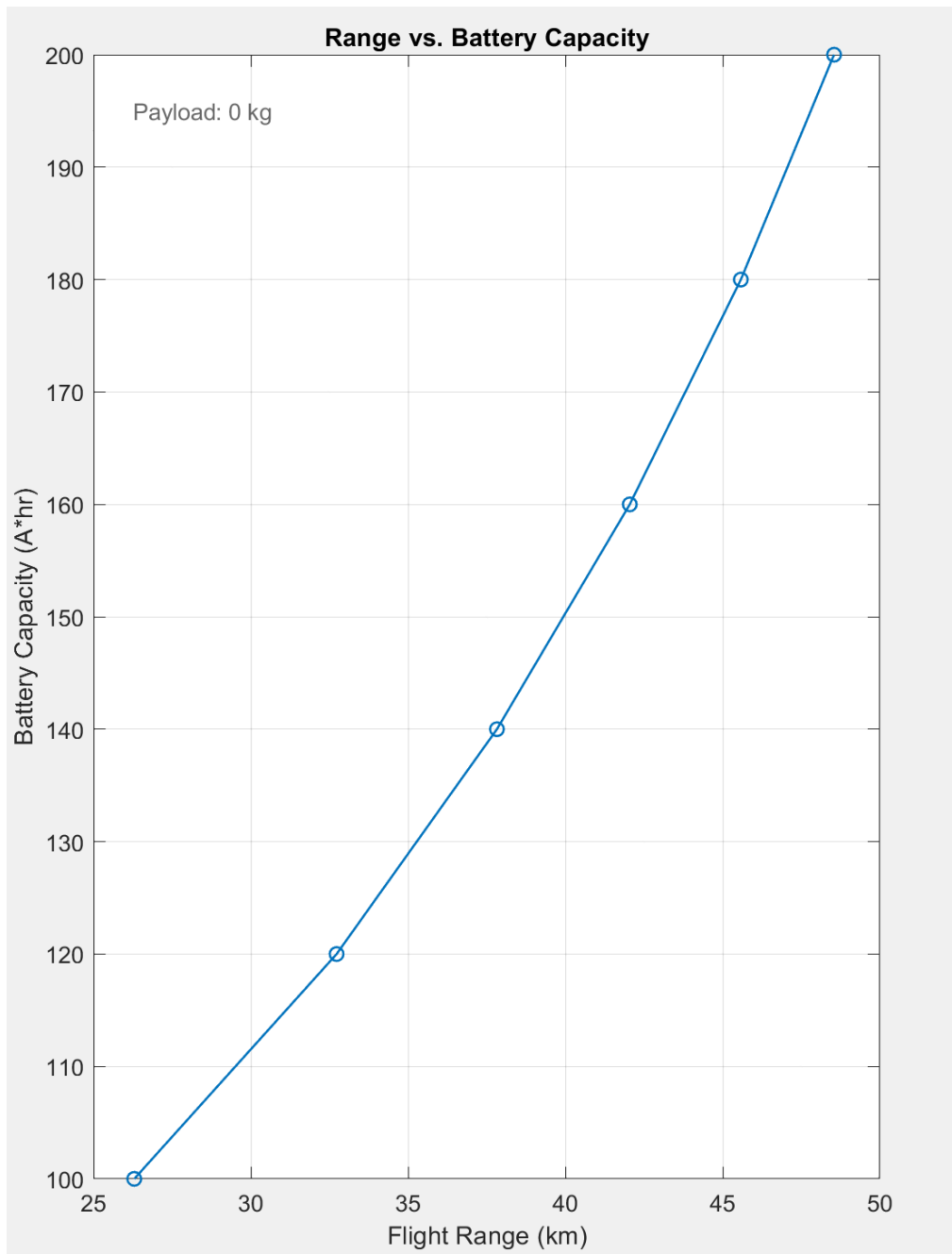


Figure 3.13 Range vs. Battery Capacity Li-Sulfur Battery

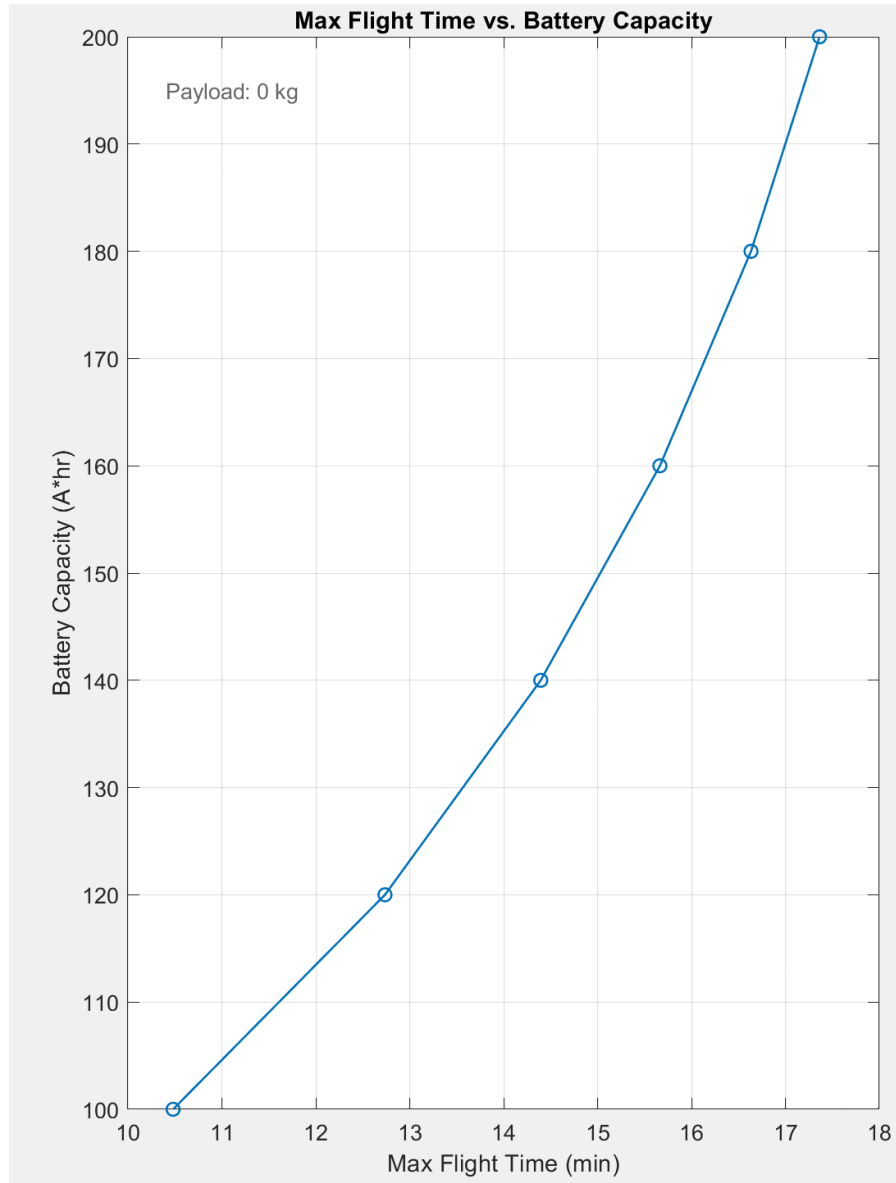


Figure 3.14 Max Flight Time vs. Battery Capacity Li-ion Battery

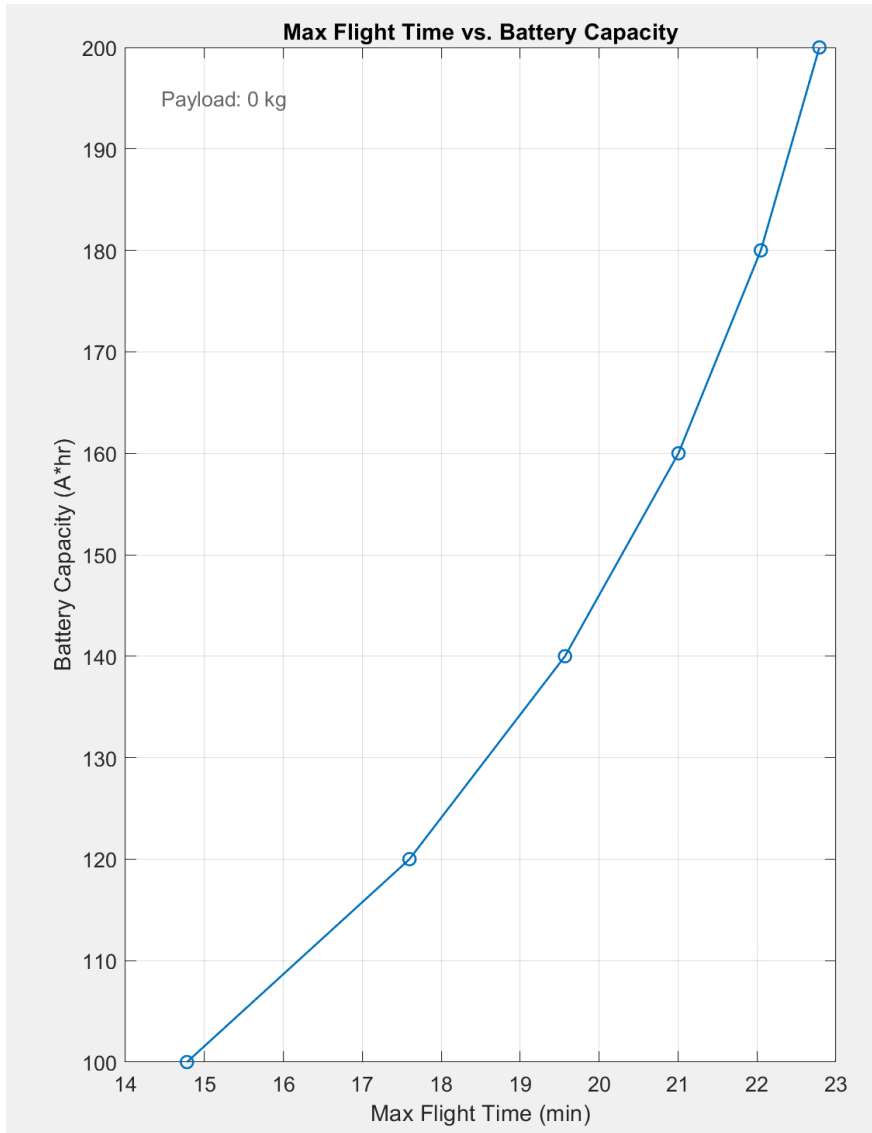


Figure 3.15 Max Flight Time vs. Battery Capacity Li-Sulfur Battery

In the above four graphs, we can see an increase in the maximum flight time as well as range for the aircraft that is powered with Li-S battery as opposed to traditional Li-ion.

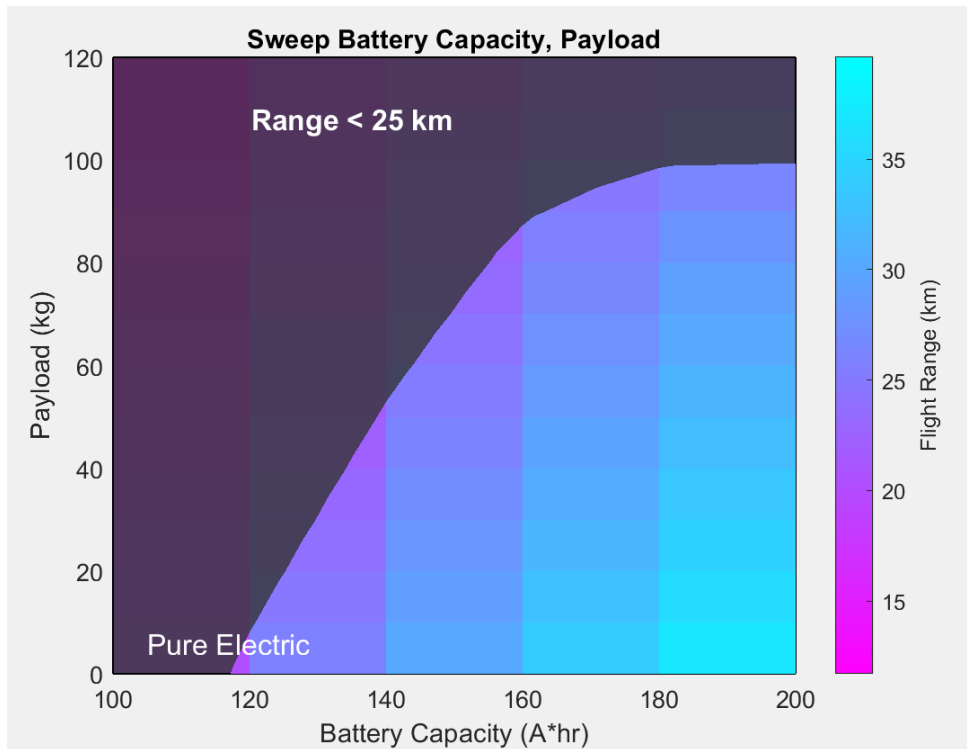


Figure 3.16 Sweep Battery Capacity Li-ion

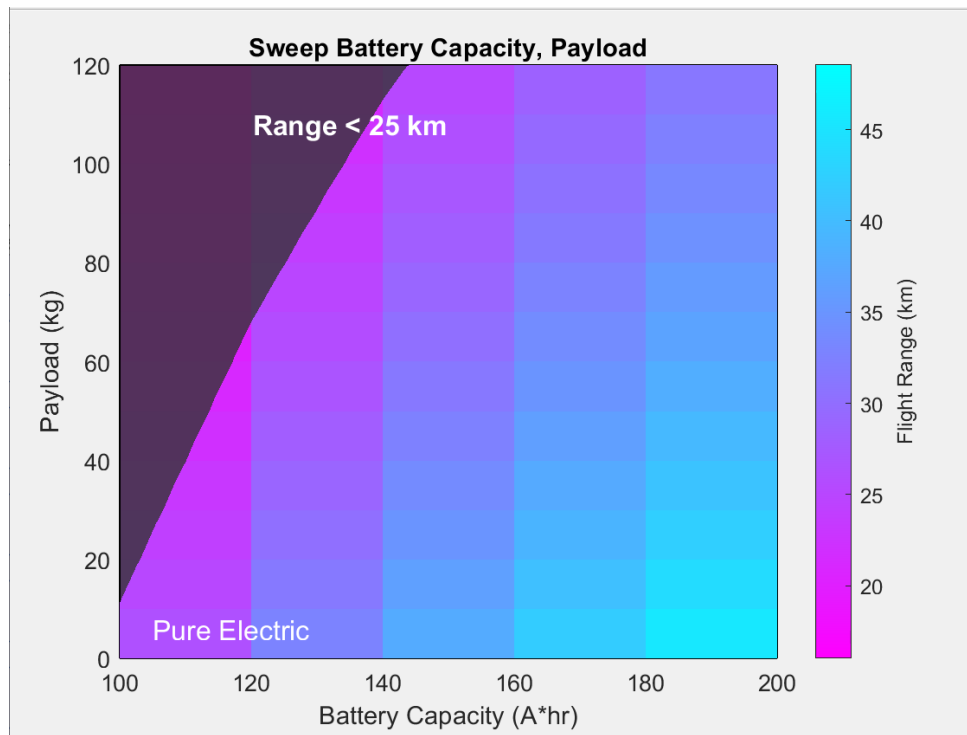


Figure 3.17 Sweep Battery Capacity Li-Sulfur

The last graph for comparison shows the difference in safety operating zones for the two battery chemistries. Li-S performs better in terms of range as well as payload as shown in figures 3.13 and 3.14.

CHAPTER FOUR

LITHIUM SULFUR BATTERY MODEL SUBSYSTEM

4.1 Introduction to Simulink Model

The evolution of battery technologies has seen rapid advances, particularly in the domain of lithium-sulfur (Li-S) batteries due to their potential for high energy densities and sustainability. However, accurately representing the intricate phenomena such as dendrite growth and the shuttle effect within these batteries has been a significant challenge in the research community.

4.1.1 Purpose and Significance

The primary purpose of the simulations is to fill this existing knowledge gap by providing a comprehensive model that offers both a detailed and an accurate representation of the key phenomena occurring in Li-S batteries. With the rising demand for efficient and long-lasting energy storage solutions, understanding these complex processes becomes indispensable. Simulating these effects not only assists in predicting battery performance and potential failure modes but also facilitates the optimization of battery design and management systems.

The significance of these simulations extends beyond academic interests. By understanding the intricacies of dendrite growth and the shuttle effect, battery manufacturers can potentially introduce improvements in battery longevity, safety, and efficiency. This has broader implications for industries relying on battery technologies, including electric vehicles, renewable energy storage, and consumer electronics.

4.1.2 Brief Overview of the Model's Intent to Represent Dendrite Growth and the Shuttle Effect

The model is a novel attempt to capture the nuances of Li-S battery behavior, with a keen focus on two critical phenomena: dendrite growth and the shuttle effect.

- **Dendrite Growth:** Dendrites are tiny, needle-like structures that grow on the battery's lithium electrode during charge and discharge cycles. Their growth can pierce the separator, leading to internal shorts, reduced battery life, and potential safety hazards.

The model aims to simulate the onset and progression of dendrite formation, allowing for a predictive understanding of its impact on battery performance. [21]

- **Shuttle Effect:** This refers to the movement of dissolved lithium polysulfides between the battery's electrodes. While it is a natural occurrence in Li-S batteries, excessive shuttling can lead to rapid capacity fade and reduced battery efficiency. Our model incorporates mechanisms to represent the shuttle effect, emphasizing its relationship with battery performance metrics. [22]

This simulation is designed to be a pivotal step forward in the realm of Li-S battery research, providing insights that could revolutionize the way we perceive, design, and utilize these batteries in the future.

4.2 Model Development and Configuration

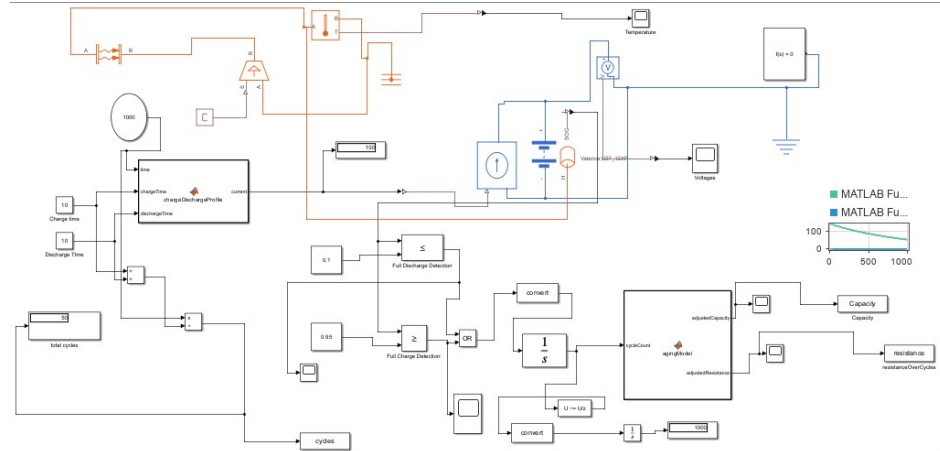


Figure 4.1: Simulink Model of Battery

4.2.1 Brief Description of Model's Architecture

1. Input and Control Subsystem:

- Charge/Discharge Profile: Blocks labeled "Charge Time" and "Discharge Time" determine the duration of each phase.
- Total Cycles: Defines the number of charge-discharge cycles the battery undergoes.

2. Battery Dynamics and Monitoring (Central Section):

- Dynamics: The central section represents the core electrochemical dynamics. The interconnected blocks could model ion transport, reactions, and overall battery behavior.
- Monitoring: Blocks such as "Voltage" and "Capacity" indicate real-time tracking of the battery's performance metrics.

3. Feedback and Safety Systems:

- "Full Charge Detection" and "Full Discharge Detection" are safety mechanisms ensuring the battery doesn't overcharge or excessively discharge.

2. Charge discharge Detection:

These blocks detect when the battery is fully charged or fully discharged. When either condition is met, an output signal is generated. The "OR" block ensures that an output signal is generated for either of the conditions.

- Full charge detection: operator detect each full charge detection if SOC values downs to 0.1 or 10%
- Full Discharge Detection: operator detect each full charge detection if SOC values become greater than to 0.95 or 95%
- 1/S (Integration Block):
- This block integrates the incoming signal. Given the context, it keeps a cumulative count of charge/discharge cycles the battery undergoes. Batteries typically have a certain number of cycles before they experience significant degradation.

3. Cycling Control:

- Total cycles: Total number of cycles the system will be calculated with

$$\text{Number of cycles} = \frac{\text{Total charging time} + \text{Total discharging time}}{\text{Stop time}}$$

(6)

- Cycles: this block keep calculate of the number of completed cycles in given amount of time.

4.2.2 Battery Model

To create the Lithium-Sulfur Battery, here is a breakdown of the mentioned properties needed to replicate the chemistry.

1. Custom Component: Lithium-Sulfur (Li-S) Battery (Table-Based)

Properties:

2. Type of Battery: Lithium-Sulfur (Li-S)

3. Capacity (Ah):

- Value: 144 Ah

This value indicates the total amount of electric charge the battery can deliver at the rated voltage on a full charge. In this case, the Li-S battery can deliver a current of 144 amperes for 1 hour before it is completely discharged.

4. Nominal Voltage (V):

- Value: 13.6 V

Nominal voltage is the rated voltage of the battery. For this Li-S battery, it's 13.6 volts, which is typically the average voltage the battery will hold over its discharge curve. [19]

5. Energy (Wh):

- Value: $144Ah \times 13.6V = 1958.4Wh$

This value gives the total energy storage capacity of the battery. It's calculated by multiplying the capacity in Ah with the nominal voltage in V. In this case, the Li-S battery can store 1958.4 watt-hours of energy.

4.2.3 Voltage Sensor (V)

Located on the right side, the voltage sensor is connected to the main circuit to measure the voltage across the terminals of the battery. Its purpose is to give a signal representative of the battery's voltage. This can be used for monitoring, control purposes, or even for safety checks (such as ensuring voltage doesn't exceed or go below certain levels).

4.2.4 Controlled Current Sensor (I)

This block measures the current flowing through the battery. Unlike a regular current sensor, a "controlled" version may allow for a specific condition or threshold to be set. When the current reaches this condition/threshold, the sensor may send a signal or trigger an event. Monitoring the current is crucial for several reasons:

- Safety: Excessive current can cause overheating or other damage.
- State of Charge: The current can be integrated over time to calculate the charge or discharge amount, helping in determining the battery's state of charge.

4.3 Temperature Mechanism

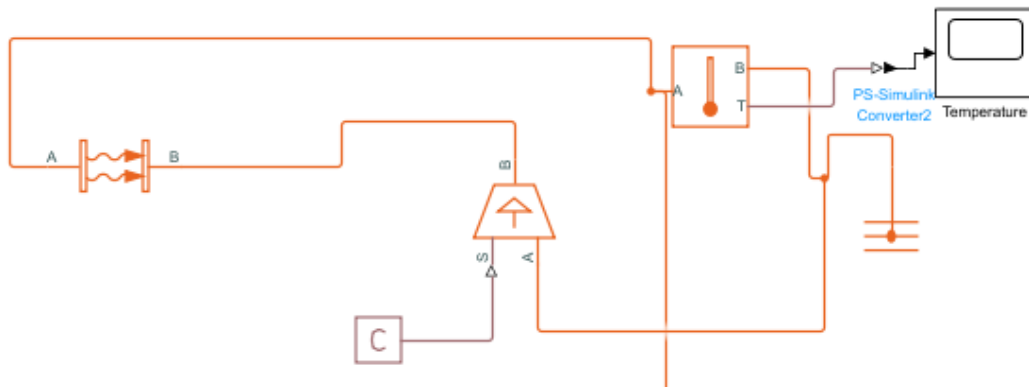


Figure 4.2: Temperature Mechanism within Battery Model

To further delve into the temperature mechanism within the battery model, it is important to understand each block within the model. To cover this, detailed overview of components and their interactions in the temperature mechanism:

1. Controlled Temperature Source:

- This component generates a controlled temperature. The control is likely dictated by the input it receives on its "S" port.
- The "S" port of the Controlled Temperature Source is connected to a PS Constant, which provides a set or reference temperature. The temperature source will try to maintain or react based on this constant value.
- The controlled temperature source is grounded, providing a reference or zero point for the temperature measurements.

2. Temperature Sensor (A):

- This component is directly connected to the thermal port of the battery. Its primary function is to measure the temperature of the battery and provide a signal representative of that temperature.
- The output from the temperature sensor is fed into the Convective Heat Transfer block. This suggests that the temperature sensor's readings are used to determine how much heat needs to be transferred (or convected) away from the battery.

3. Convective Heat Transfer (AB):

- Convective heat transfer involves the transfer of heat through a fluid (like air) due to the fluid's motion. In this model, it's likely simulating how heat is transferred away from the battery (based on the battery's temperature) into the surrounding environment or a cooling medium.

- The input to this block is the temperature reading from the Temperature Sensor. Thus, the heat transfer rate will be dependent on the current temperature of the battery.
- The output from this block is grounded, which might represent the dissipation of the transferred heat to the surrounding environment.
- The other side of the Convective Heat Transfer block connects to the Controlled Temperature Source, suggesting an interaction or feedback mechanism between the heat being generated and the heat being transferred.

4. PS-Simulink Converter → Temperature (B):

- This component converts the physical signal of temperature into a Simulink signal. It takes the output from the Convective Heat Transfer block, which represents the rate or amount of heat being transferred away from the battery.
- The Simulink signal can then be used for further analysis, visualization (using a scope), or control within the Simulink environment.

This temperature mechanism is a feedback system that monitors the battery's temperature, determines the amount of heat to be transferred away from the battery based on this temperature, and potentially controls the temperature using the Controlled Temperature Source. The system ensures that the battery's temperature remains within desired limits, and any excess heat is convected away efficiently. The PS-Simulink

Converter allows for real-time monitoring and analysis of the temperature dynamics within a Simulink environment.

4.4 Charging and Discharging Profile Mechanism

The next step to understanding the battery model is to delve into the charge and discharge profile mechanism based on the provided block diagram and the associated code.

1. Inputs:

- The function block **chargeDischargeProfile** takes in three parameters: **time**, **chargeTime**, and **dischargeTime**.
- **time**: Represents the current simulation time.
- **chargeTime**: The duration for which the battery should be charged.
- **dischargeTime**: The duration for which the battery should be discharged.

2. Profile Generation:

- The function defines two constants: **CHARGE_CURRENT** and **DISCHARGE_CURRENT**, representing the charging and discharging rates respectively.
- The sum of **chargeTime** and **dischargeTime** gives a **CYCLE_TIME**, which represents one complete charge-discharge cycle.
- The function then calculates the current cycle number based on elapsed time using the expression

$$\text{Number of cycles} = \frac{\text{Total charging time} + \text{Total discharging time}}{\text{Stop time}}$$

(7)

This effectively quantizes the continuous time input into discrete charging and discharging periods.

- Subsequently, the function determines where the current time lies within the current cycle using the expression **mod(time, CYCLE_TIME)**. This gives the phase or portion of the cycle we're currently in.

3. Current Determination:

- Based on the phase of the current cycle determined from the mod operation, the function checks whether we are in the charging or discharging phase.
- If the current phase is less than **chargeTime**, the function returns **CHARGE_CURRENT**, indicating that the battery is being charged.
- If the current phase exceeds **chargeTime**, the function returns **DISCHARGE_CURRENT**, implying that the battery is in the discharging phase.

4. Purpose:

The primary purpose of the **chargeDischargeProfile** function block is to generate a current profile that simulates a repetitive charging and discharging pattern of a battery based on the defined charge and discharge durations. This is beneficial in various scenarios:

- **Testing Battery Behavior:** This allows users to simulate how a battery would perform under periodic charging and discharging scenarios, helping to analyze its behavior, capacity retention, efficiency, and other parameters.

- **Aging and Life Cycle Analysis:** By simulating multiple charge-discharge cycles, this block can be instrumental in studying the aging effects on the battery, as well as estimating its overall lifespan.
- **Integration with Controlled Current Source:** The generated current profile feeds into a controlled current source connected to the battery. This source will ensure the battery is charged or discharged according to the profile, making the simulation more realistic.

The **chargeDischargeProfile** function block creates a periodic current profile based on specified charge and discharge durations, enabling a systematic and repetitive charging and discharging simulation of a battery.

4.5 Dendrite Growth and Shuttle Effect Representation

Dendrites are microscopic, conductive fibers that grow inside a battery, especially in lithium-ion batteries. As these dendrites grow, they can cause internal short circuits, which can reduce the battery's capacity and increase its internal resistance. [21] Over time, as the number of charge-discharge cycles increases, the growth of dendrites can become more pronounced, potentially leading to a faster decrease in capacity and an increase in internal resistance.

The shuttle effect refers to the movement of active material between the anode and cathode of a battery. This movement can cause a loss of active material, which can lead to a reduction in capacity. [22] Similar to dendrite growth, the shuttle effect can become more pronounced over time, leading to a more significant decrease in capacity with each charge-discharge cycle.

To calculate the impact of these effects over time, it is important to define the aging model equations appropriately.

1. Define the Aging Model Equations:

- For each cycle, the battery's capacity might decrease by a certain percentage due to dendrite growth and the shuttle effect. Similarly, the resistance might increase by a specific percentage.

$$\begin{aligned}
 & \textit{capacity}_{\textit{next_cycle}} \\
 &= \textit{capacity_current_cycle} \times (1 - \textit{dendrite_growth_rate} \\
 &\quad - \textit{shuttle_effect_rate})
 \end{aligned}
 \tag{8}$$

$$\begin{aligned}
 & \textit{resistance}_{\textit{next_cycle}} \\
 &= \textit{resistance_current_cycle} \times (1 \\
 &\quad + \textit{dendrite_resistance_increase_rate})
 \end{aligned}
 \tag{9}$$

The second step is to calculate the capacity and resistance for each subsequent cycle based on the previous cycle's values are calculated using a loop or iterative method.

4.5.1 Aging Model

1. Aging Model:

- **Input - cycleCount:** This represents the total number of charge/discharges cycles the battery has undergone. The more cycles a battery goes through, the more it ages.

- **Outputs - adjustedCapacity & adjustedResistance:** As a battery ages, its total available capacity typically decreases, and its internal resistance increases. The aging model will adjust these parameters based on the number of cycles and potentially other internal factors related to dendrite growth and the shuttle effect.
- **Dendrite Growth:** Over time, lithium can form metallic structures called dendrites. These dendrites can grow and bridge the gap between the anode and cathode, leading to a short circuit. This increases the internal resistance of the battery and poses a risk of failure.
- **Shuttle Effect:** This refers to the movement of lithium ions between the anode and cathode without them participating in charge or discharge reactions. This can result in a loss of active lithium, reducing the capacity of the battery.

2. Capacity & Resistance Blocks:

- The adjusted values from the aging model feed into these blocks. They represent the current available capacity of the battery and its internal resistance at any given point in time. The adjusted resistance, for instance, would increase over time due to the effects of dendrite growth.

As the battery undergoes charge/discharge cycles, the aging model takes into account the detrimental effects of Dendrite growth and the shuttle effect, adjusting the available capacity and internal resistance of the battery over time. This provides a more realistic simulation of battery behavior as it ages.

4.6 Simulation Results Model Development and Configuration

4.6.1 Voltage Output

From the graph and given input conditions, this shows a repetitive charging and discharging pattern of the battery. The graph represents the voltage output as recorded by a voltage sensor over a set duration.

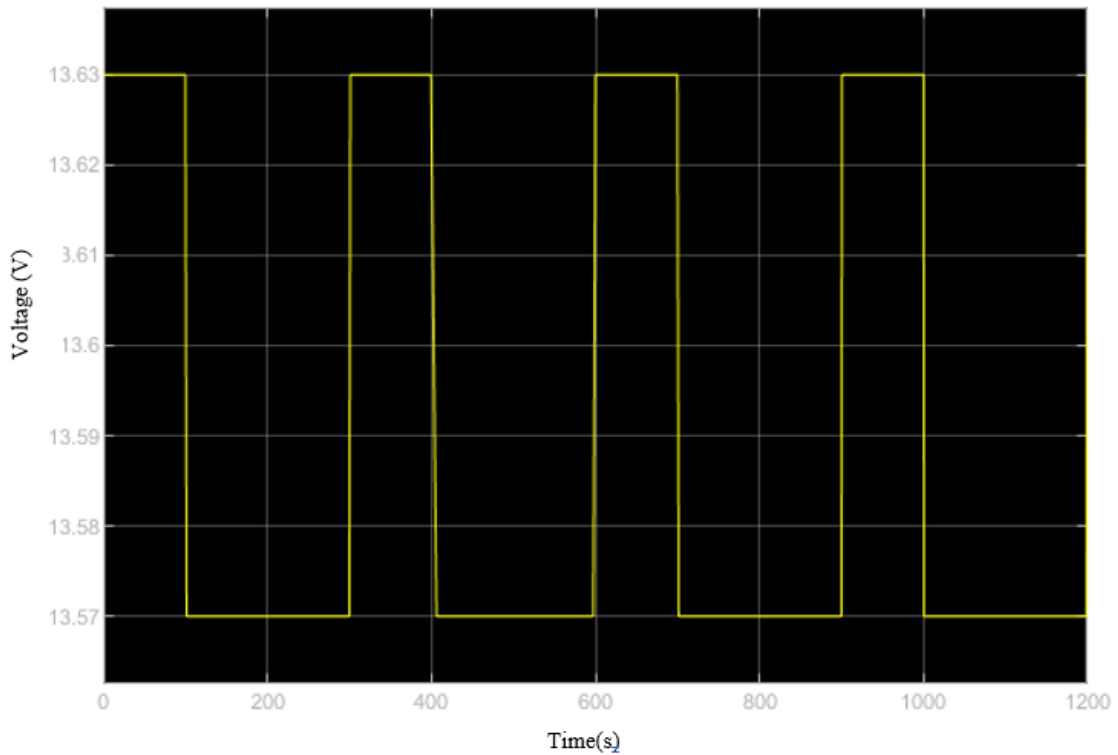


Figure 4.3: Voltage Fluctuation over Multiple Charge Cycles

To further breakdown of the graph based on input conditions:

1. Charging Phase: The upward slope on the graph indicates the charging phase. It lasts for 100 seconds, as specified by the "charging time". The voltage appears to increase rapidly during this phase.
2. Discharging Phase: After the charging phase, there's a period of steady decline, which is the discharging phase. This lasts for 200 seconds, as per user input.

3. Rest or Idle Phase: Between the cycles, there seems to be a relatively stable voltage, which represents an idle phase or a period where the system is being charged or discharged actively. The time it stays at this level is the difference between the total cycle time (charging time + discharging time = 300 seconds) and the time until the next charge starts.
4. Total Cycles: Based on the graph and the input that there are a total of 4 cycles, four distinct patterns of charging and discharging can be observed over the span of the simulation.
5. Stop Time: The simulation to stop at around 1200 seconds, as indicated. By that time, all 4 cycles (each lasting 300 seconds for a total of 1200 seconds) would have been completed.
6. Voltage Levels: The maximum and minimum voltage levels can also be observed. The system seems to charge up to around 13.63 volts and discharges to approximately 13.57 volts, indicating a small voltage range of variation during the cycles.

The graph provides a visual representation of a system being charged and discharged over time. The repetitive patterns confirm the cyclic nature of the process, and the time intervals on the x-axis correlate with the input conditions provided for charging, discharging, and total simulation time.

4.6.2 Capacity

From the graph, the relationship between the capacity of the battery and the number of charge-discharge cycles it has undergone are shown.

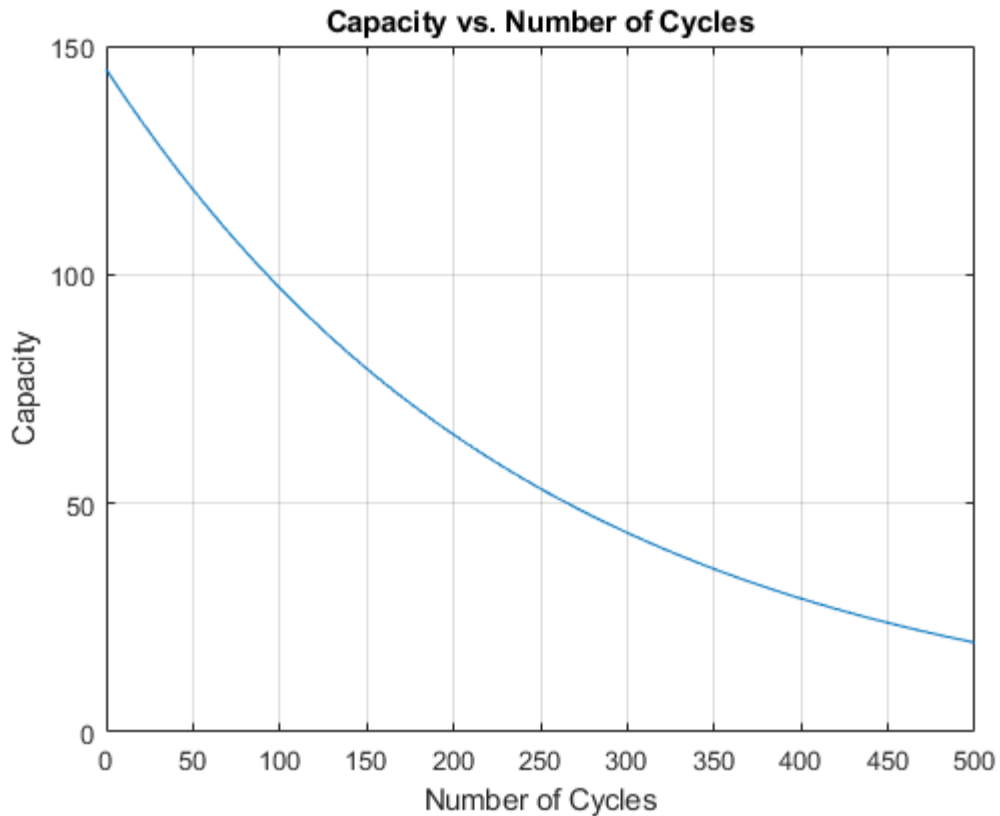


Figure 4.4: Capacity vs Number of Cycles

1. Declining Capacity:

- The battery's capacity decreases as the number of cycles increases. This decline in capacity over cycles is a common phenomenon in Lithium Sulfur Batteries.
- The graph indicates that as the battery undergoes more charge-discharge cycles, its ability to hold and deliver its full original capacity diminishes.

2. Initial Capacity:

- At cycle 0 (i.e., when the battery is brand new or hasn't been cycled), the battery's capacity is at its maximum, which is 144Ah.

3. Rate of Capacity Fade:

- The capacity fade seems to be more pronounced during the initial cycles, as indicated by the steeper slope at the start. This suggests that the battery loses capacity at a faster rate in its early life.
- As the number of cycles increases, the rate of capacity decline becomes more gradual, suggesting that while the battery continues to lose capacity, it does so at a slower pace in its later life.

4. End of Life:

- By the time the battery reaches around 500 cycles, its capacity is just above 0, indicating it has nearly reached its end of life and can't hold much charge anymore.

5. Overall Trend:

- The curve is concave, suggesting a non-linear decrease in capacity with cycles. This might be indicative of certain chemical and physical processes within the battery which cause a more rapid decline initially, followed by a slower decrease as the battery ages.

This graph provides a visual representation of how the capacity of a battery degrades over a specified number of charge-discharge cycles. It's a typical representation used to understand and predict the lifespan and performance of batteries.

4.6.3 Resistance

The graph illustrates the relationship between the internal resistance of a battery and the number of charge-discharge cycles it has undergone.

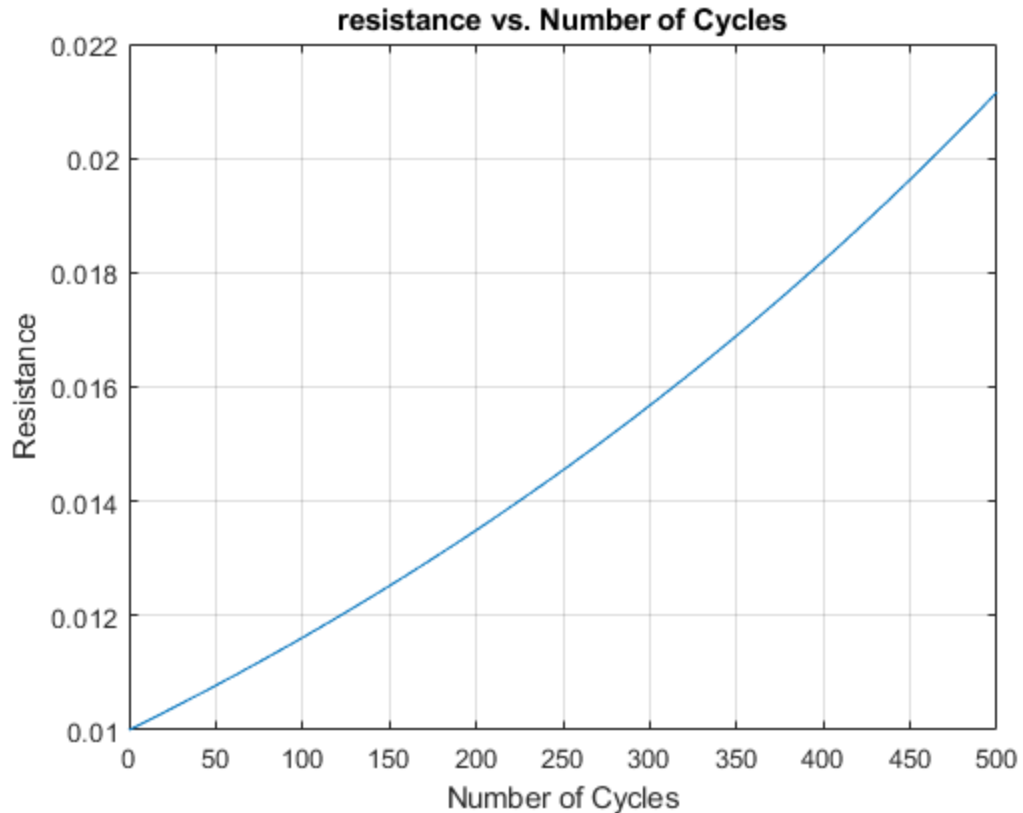


Figure 4.5: Internal Resistance per Cycle

1. Increasing Resistance:

- As the battery undergoes more charge-discharge cycles, its internal resistance increases. An increase in internal resistance is common for Li-S batteries as they age.
- The rise in resistance indicates that the battery becomes less efficient over time. A higher internal resistance means more energy is lost as heat during charging and discharging, which can reduce the overall efficiency of the battery and result in increased operating temperatures.

2. Initial Resistance:

- At cycle 0, the battery's resistance is at its lowest, which is close to 0.01 ohms.

3. Rate of Resistance Increase:

- The resistance seems to increase exponentially with the number of cycles. This increase suggests a consistent rate of degradation in terms of resistance as the battery is used.
- This consistent rise might be due to the gradual buildup of unwanted compounds or changes in the battery's internal structure over time.

4. End Resistance:

- By the time the battery reaches around 500 cycles, its resistance appears to be slightly above 0.021 ohms, indicating a measurable increase from its starting resistance.

5. Overall Trend:

- The graph is exponentially increasing indicating a consistent increase in resistance with the number of cycles. There is an accelerating trend in resistance increase.

This graph provides insight into how the internal resistance of a battery evolves over a specified number of charge-discharge cycles. An increase in resistance over time can impact the battery's performance, leading to reduced capacity, longer charging times, and potential heating issues. This is very common in Li-S batteries as the dendrite growth and polysulfide shuttle effect impact internal resistance. Monitoring and understanding resistance changes can be crucial for assessing battery health and predicting its useful lifespan.

4.7 Comparison with Lab Data

For this dissertation, lab data from a now defunct manufacturer of Li-S cells was used. Through careful analysis of lab data for a lithium-sulfur battery, I was pleased to observe a strong correlation with my simulation results. Both datasets clearly demonstrated the expected trends of capacity decrease and resistance increase within the battery. This consistency between the experimentally obtained data and the simulation output reinforces the validity of my model. It further suggests that the simulation accurately captures the fundamental electrochemical processes governing lithium-sulfur battery behavior.

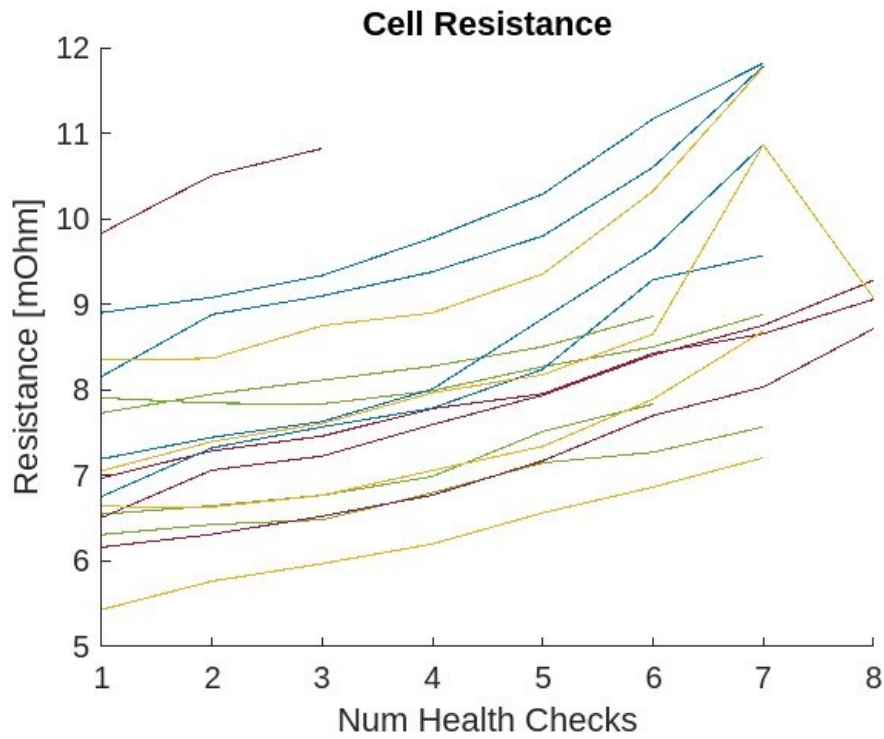


Figure 4.6: Cell Resistance Lab Data

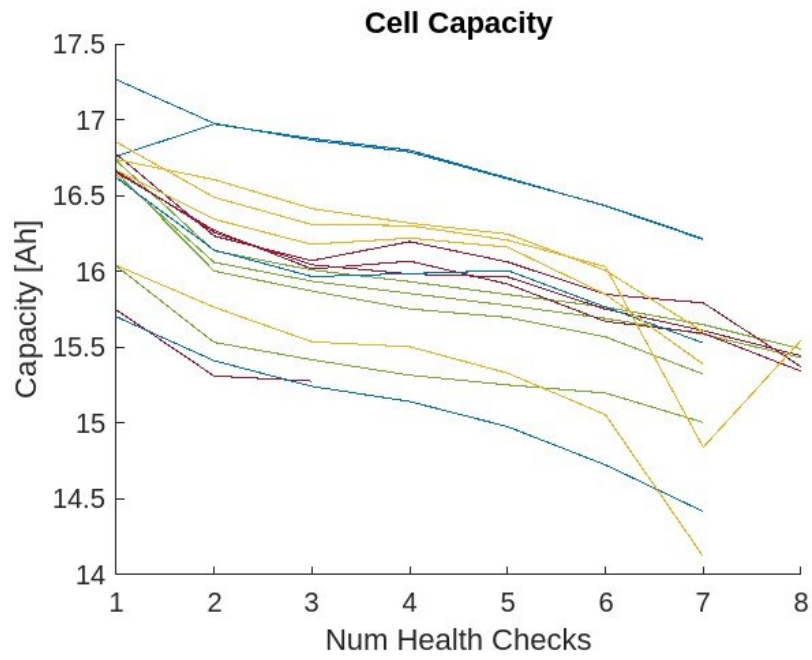


Figure 4.7: Cell Capacity Lab Data

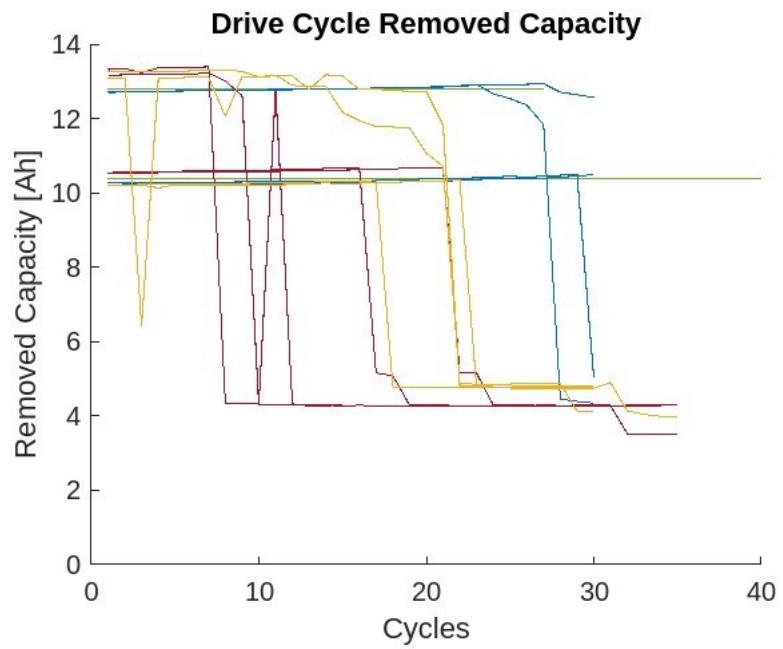


Figure 4.8: Drive Cycle Removed Capacity Lab Data

These graphs provide compelling evidence for the agreement between the lab data and simulation results. The observed increase in resistance aligns with the limitations caused by the formation of insulating polysulfides during battery operation. Similarly, the decline in capacity reflects the loss of active sulfur material and reduced accessibility of reaction sites. Furthermore, the decrease in drive capacity underscores the practical impact of these changes, directly affecting the battery's ability to power a device. Overall, this strong correlation across multiple parameters solidifies the simulation's ability to model real-world lithium-sulfur battery behavior.

4.8 Conclusion

Through comprehensive simulations, the model has revealed the nuanced effects of dendrite growth and the shuttle effect on battery performance over time. The results have demonstrated a consistent decrease in battery capacity and a concurrent increase in internal resistance as the number of charge-discharge cycles progresses. These effects become particularly pronounced after a specific cycle threshold, emphasizing the detrimental role of dendrite growth and the shuttle effect in battery degradation.

What sets this model apart is its novel representation of these two phenomena. While many models provide a generic overview of battery aging, this model delves deep into the microscopic interactions taking place within the battery, especially concerning dendrite formation and the movement of active material. This granularity not only enhances the accuracy of predictions but also offers insights into potential mitigation strategies.

In essence, this model serves as a pivotal tool for battery researchers in both an academic setting as well as industry. It emphasizes the need for innovative

solutions to combat dendrite growth and the shuttle effect, ensuring the longevity and safety of batteries in various applications.

CHAPTER FIVE
MODEL PREDICTIVE CONTROL AND LINEAR QUADRATIC REGULATOR
IMPLEMENTATION

5.1 Control Design and Simulation

In this chapter, the intricacies of control design and simulation methodologies tailored for electric air taxi systems are explored, focusing on the integration of Model Predictive Control (MPC) algorithms for thrust management. With the foundational understanding established in the literature review, attention turns towards the practical implementation of MPC-based thrust control systems. The fundamental principles of MPC are examined, the architectural framework of the control system is elucidated, and the selection and integration of dynamic models necessary for simulation are outlined. Furthermore, the intricacies of MPC algorithms, their adaptability to electric air taxi flight dynamics, and the considerations involved in the development of a robust control strategy are discussed. Through a comprehensive examination of control design and simulation methodologies, the groundwork is laid for the subsequent evaluation and analysis of MPC-based thrust control in electric air taxi systems.

5.1.1 System Overview

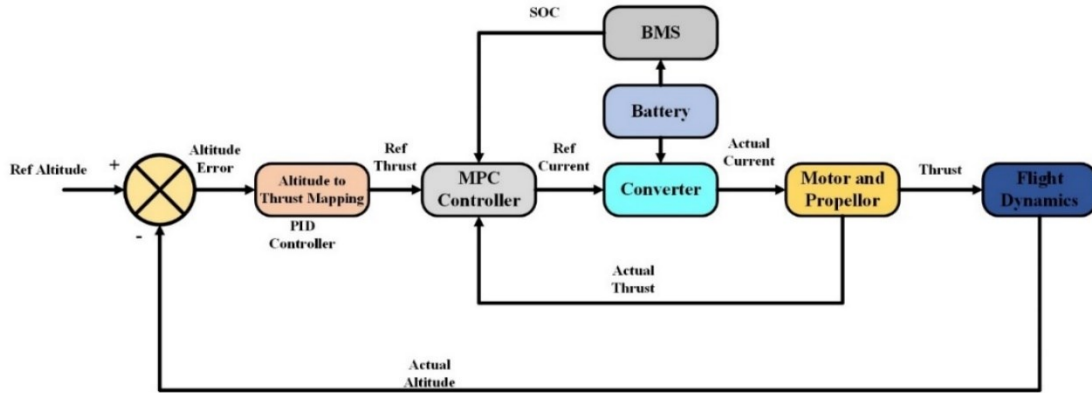


Figure 5.1: Complete Block Diagram of System

The complete block diagram of the system is shown in the figure above.

The flight altitude error is a pivotal parameter in the control system of the electric air taxi aircraft, serving as a crucial input to ensure stable and precise flight operations. In the integrated control architecture, the altitude error is channeled into a Proportional-Integral-Derivative (PID) controller, which acts as a primary component responsible for mapping the altitude error to a reference thrust output. This PID controller operates based on the difference between the desired altitude and the actual altitude of the electric air taxi aircraft. By continuously monitoring and adjusting this error signal, the PID controller aims to maintain the electric air taxi at its designated altitude, contributing to stable flight dynamics.

The reference thrust generated by the PID controller serves as a target output for the aircraft's propulsion system. It represents the desired amount of thrust required to achieve and maintain the specified altitude. The PID controller calculates the reference thrust based on the magnitude and direction of the altitude error, employing proportional, integral, and derivative control actions to ensure precise and responsive altitude regulation.

In conjunction with the PID controller, the Model Predictive Control (MPC) controller plays a critical role in fulfilling the reference thrust generated by the PID controller. The MPC controller operates in a predictive manner, leveraging advanced algorithms to anticipate future system behavior and optimize control inputs over a finite time horizon. In the context of altitude control, the MPC controller adjusts the reference thrust output to account for dynamic changes in environmental conditions, aircraft weight, and other pertinent factors affecting flight performance.

One key aspect of the MPC controller is its integration with the State of Charge (SOC) information obtained from the Battery Management System (BMS). The SOC serves as a critical parameter in determining the available energy reserves of the onboard battery pack. By incorporating SOC data into its control algorithms, the MPC controller can effectively manage energy consumption and optimize the utilization of available battery capacity. This integration enhances the efficiency and endurance of the electric air taxi aircraft, enabling longer flight durations and increased operational range.

Upon receiving the reference thrust command from the MPC controller, the propulsion system of the electric air taxi aircraft is activated to generate the required thrust output. The reference thrust is translated into a corresponding reference current signal, which is then fed into the converter unit responsible for regulating the power supplied to the aircraft's electric motors. The electric motors, in turn, convert electrical energy into mechanical thrust, propelling the electric air taxi aircraft and enabling it to ascend, descend, or maintain its altitude as commanded by the control system.

The integrated control architecture described above exemplifies the sophisticated and coordinated approach employed in the operation of electric air taxi

aircraft. By combining PID control for altitude regulation with MPC-based thrust management and SOC-aware energy optimization, the control system enables precise, efficient, and reliable flight operations in diverse environmental conditions. Furthermore, the integration of advanced control algorithms and battery management strategies underscores the continuous advancements in electric air taxi technology aimed at enhancing safety, performance, and sustainability in urban air mobility applications.

5.1.2 Converter Modeling

The buck converter plays a pivotal role in fulfilling the current requirement necessary for the electric motor to generate thrust in an electric air taxi aircraft. As the electric air taxi ascends, descends, or maintains its altitude, the motor requires varying levels of electrical current to produce the desired thrust output. The buck converter serves as an intermediary between the power source, typically a battery pack or power distribution system, and the electric motor, regulating the voltage and current supplied to the motor to meet the dynamic demands of flight operations.

Operating on the principle of pulse-width modulation (PWM), the buck converter adjusts the duty cycle of its switching elements to regulate the output voltage and current levels. During flight, the control system continuously monitors the reference thrust command generated by the Model Predictive Control (MPC) algorithm. Based on this command, the control system calculates the corresponding reference current required to achieve the desired thrust output.

The buck converter then modulates the input voltage from the power source to deliver the precise current level demanded by the motor. By converting excess voltage into controlled current flow, the buck converter optimizes energy efficiency and

minimizes power losses, ensuring that the motor operates within its specified operating parameters. This dynamic control of current flow enables the electric motor to respond rapidly to changes in altitude or flight conditions, facilitating smooth and stable flight maneuvers while conserving energy resources. The circuit of buck converter is shown in the figure 5.2.

Ideally, it is considered that the inductor and the capacitor will act as their ideal property, which means they will only oscillate the power but not dissipate on themselves. But this does not happen in practice. In this case, the output voltage will experience the impedance of the inductor in series with load and effective series resistance (ESR) of the capacitor parallel to load. This ESR will introduce the zero in the model of the buck converter which will disturb the response of the system. We have to model such parasitic impedances in order to get results near to a real case scenario. In the ‘on’ state the diode will act as an open circuit and the switch will act as a closed circuit, but it’s ‘on’ state resistance will appear in series with the inductor impedance. The ‘on’ state resistance usually is not a huge or prominent resistance. It will not affect the system. The following figure shows the ‘on’ state circuit of the buck converter.

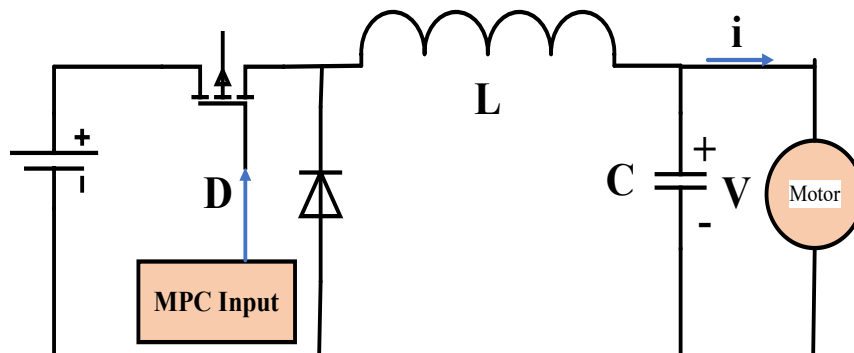


Figure 5.2 Buck Converter

The capacitor impedance and ESR are in series and the Load resistance is in parallel fashion so the equivalent resistance will be:

$$R_{eq} = R_{lo} \parallel \left(\frac{C}{S} + R_c \right)$$

$$R_{eq} = \frac{R_{LO}C + R_{LO}R_C S}{(R_{LO} + R_C)S + C}$$
(10)

$$V_0 = \frac{\frac{R_{LO}C + SR_{LO}R_C}{(R_{LO} + R_C)S + C} V_S}{\frac{V_S R_{LO}C + SR_{LO}R_C}{(R_{LO} + R_C)S + C} + R_{dson}LS + R_L}$$
(11)

The final transfer function will be:

$$\frac{V_0}{D(S)} = \frac{(R_{LO}C + SR_{LO}R_C)V_S}{(R_C L + LR_{LO})S^2 + (R_{LO}R_C + LC + R_{dson}R_{LO} + R_{LO}R_L + R_{dson}R_C + R_L R_C)S + R_{LO}C + R_{dson}C + R_L C}$$
(12)

The following table shows the abbreviation of each variable.

Table 2 Abbreviations of Each Variable

Sr #	Variable	Detail
1	V_0	Output voltages
2	R_C	ESR of Capacitor
3	R_{LO}	Load Resistance
4	R_{dson}	Switch on resistance

Table 2 – Continued

5	R_L	Inductance impedance
6	$D(S)$	Duty Cycle
7	V_S	Input voltages
8	L	Inductance
9	C	Capacitance

5.1.3 Motor Modeling

This application is considering the BLDC motor. Brushless DC (BLDC) motors offer several distinct advantages that make them well-suited for electric air taxi applications. Firstly, BLDC motors are known for their high power-to-weight ratio, making them ideal for aircraft propulsion systems where weight is a critical factor. The compact and lightweight design of BLDC motors allows for efficient use of onboard space and contributes to the overall payload capacity of the electric air taxi aircraft. This lightweight construction is especially advantageous in electric air taxi systems, where the emphasis is on maximizing payload capacity while adhering to strict weight limitations.

Secondly, BLDC motors offer precise speed and torque control capabilities, essential for maintaining stable flight dynamics and achieving precise altitude control in electric air taxi operations. The inherent design of BLDC motors, with their electronic commutation system, enables accurate and responsive control over motor speed and thrust output. This level of control is essential for electric air taxi applications, where rapid adjustments in thrust are required to counteract external disturbances, ensure

smooth takeoffs and landings, and maintain optimal flight stability throughout varying environmental conditions.

Furthermore, BLDC motors exhibit high efficiency and reliability, critical factors in the context of electric air taxi aircraft where safety and operational dependability are paramount. Compared to traditional brushed motors, BLDC motors experience less wear and tear due to the absence of brushes and commutators, resulting in reduced maintenance requirements and increased longevity. The efficiency of BLDC motors also contributes to extended flight endurance and improved energy utilization, essential considerations for enhancing the range and endurance of electric air taxi aircraft while minimizing environmental impact.

The lightweight design, precise control capabilities, and high efficiency and reliability of BLDC motors make them highly suitable for electric air taxi applications. As electric air taxi technology continues to evolve and mature, BLDC motors are poised to play a pivotal role in powering the next generation of urban air mobility solutions, offering a compelling combination of performance, efficiency, and reliability in a compact and lightweight package.

The equivalent stator circuit of a BLDC motor is shown in Figure 3.

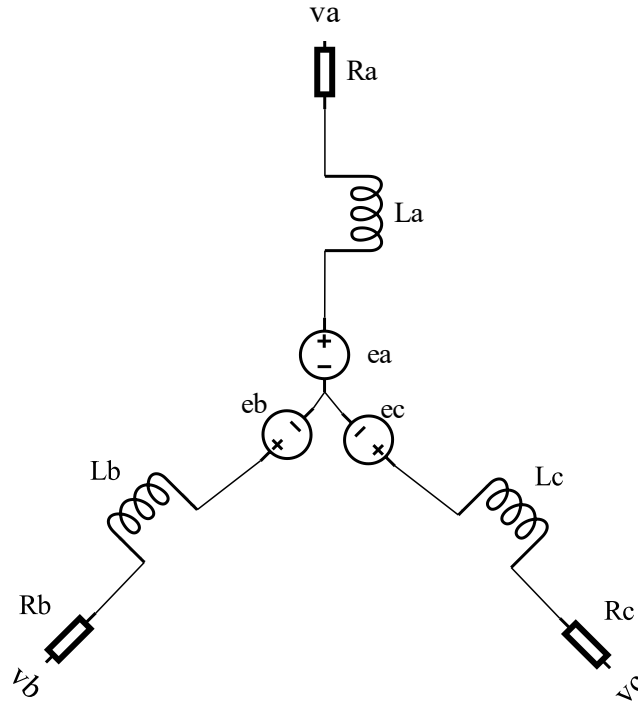


Figure 5.3 BLDC Stator Circuit

The phase Voltage equations are

$$v_a = R_a i_a + L_a \frac{di_a}{dt} + e_a \quad (13)$$

$$v_b = R_b i_b + L_b \frac{di_b}{dt} + e_b \quad (14)$$

$$v_c = R_c i_c + L_c \frac{di_c}{dt} + e_c \quad (15)$$

where

v_a, v_b, v_c are phase voltages

i_a, i_b, i_c are phase currents

R_a, R_b, R_c are phase resistances

L_a, L_b, L_c are phase inductances

e_a, e_b, e_c are back emf voltages

Since $R_a = R_b = R_c = R_s$ for a balanced three phase system and $\lambda = Li$ so equations become

$$v^{abc} = R_s i^{abc} + \frac{d\lambda^{abc}}{dt} \quad (16)$$

In order to get the state space representation of the motor. Clark Park transformation is applied

$$v^{dq0} = [T]v^{abc} \quad (17)$$

Where

$$T = \frac{2}{3} \begin{bmatrix} \cos(\theta) & \cos(\theta - 120^\circ) & \cos(\theta + 120^\circ) \\ \sin(\theta) & \sin(\theta - 120^\circ) & \sin(\theta + 120^\circ) \\ \frac{1}{2} & \frac{1}{2} & \frac{1}{2} \end{bmatrix} \quad (18)$$

Transformed equations are

$$v_d = R_s i_d + L_d \frac{di_d}{dt} - \omega L_q i_q \quad (19)$$

$$v_q = R_s i_q + L_q \frac{di_q}{dt} + \omega L_d i_d + \omega \lambda_m \quad (20)$$

After re-arranging equations

$$\begin{aligned} \frac{di_d}{dt} &= \frac{V_d}{L_d} - \frac{R_s i_d}{L_d} + \frac{\omega L_q i_q}{L_d} \\ \frac{di_q}{dt} &= \frac{V_q}{L_q} - \frac{R_s i_q}{L_q} - \frac{\omega L_d i_d}{L_q} - \frac{\omega \lambda_m}{L_q} \end{aligned} \quad (21)$$

So, the state space model of motor is

$$\begin{bmatrix} \frac{di_d}{dt} \\ \frac{di_q}{dt} \end{bmatrix} = \begin{bmatrix} -\frac{R_s}{L_d} & \frac{\omega L_q}{L_d} \\ -\frac{\omega L_d}{L_q} & -\frac{R_s}{L_q} \end{bmatrix} \begin{bmatrix} i_d \\ i_q \end{bmatrix} + \begin{bmatrix} \frac{v_d}{L_d} \\ \frac{v_q}{L_q} \end{bmatrix} + \begin{bmatrix} 0 \\ -\frac{\omega \lambda_m}{L_q} \end{bmatrix} \quad (22)$$

After getting current from this model the thrust will be

$$T = \frac{3}{2} p \lambda_m i_q \quad (23)$$

5.1.4 MPC Controller Design

The problem formulation for Model Predictive Control (MPC) involves addressing the dynamic interactions between altitude regulation, thrust management, and energy utilization while adhering to operational constraints. The objective function of the MPC controller aims to minimize deviations between the desired altitude and the actual altitude of the electric air taxi aircraft over a finite prediction horizon. This objective function may include terms that penalize altitude errors, control efforts, and deviations from desired energy utilization levels.

Constraints in the MPC problem formulation encompass limitations on altitude, thrust, and energy consumption, as well as safety and operational constraints inherent to electric air taxi flight dynamics. Altitude constraints ensure that the electric air taxi maintains safe and feasible flight altitudes, while thrust constraints regulate the maximum and minimum thrust outputs to prevent destabilizing flight conditions. Additionally, constraints on energy consumption and battery State of Charge (SOC) ensure that the electric air taxi operates within sustainable energy limits and maintains sufficient energy reserves for safe operation and emergency scenarios.

$$\text{Min} \int_0^T |T_{ref} - T_{actual}|^2 dt$$

Subject to

$$i_{min} \leq i \leq i_{max}$$

$$40\% \leq SOC \leq 100\%$$

$$h(0) = 0, \quad h(T) = H \quad (24)$$

$h(0)$ is initial altitude and $h(T)$ is final altitude and H is desired altitude.

The optimal control problem is minimizing the thrust error while maintaining the current in feasible region where the converter and motor can operate. This problem is also taking care of SOC to be maintained in a specific region. Lastly, this problem also ensure that system reaches to it desired value. When the SOC falls below from it critical limit (lower limit) then this controller will land the system.

It is crucial to land the aircraft when the State of Charge (SOC) of the battery falls below a critical value for several reasons:

Safety: Operating an electric air taxi aircraft with a low SOC poses significant safety risks. Low battery levels can lead to unexpected power loss, jeopardizing the stability and control of the aircraft during critical flight phases such as takeoff, landing, and maneuvering. Landing the electric air taxi when SOC is low mitigates the risk of in-flight emergencies and ensures the safety of passengers, crew, and bystanders.

Avoidance of Battery Damage: Allowing the SOC of the battery to deplete beyond a critical threshold can lead to irreversible damage to the battery cells. Deep discharges can cause voltage drops, chemical reactions, and structural degradation within the battery pack, reducing its lifespan and compromising its overall performance. By

landing the electric air taxi before the SOC reaches a critical level, operators can preserve the health and longevity of the battery system, minimizing maintenance costs and downtime.

Prevention of Unintended Grounding: If the SOC of the battery falls below a critical value while the electric air taxi is still airborne, there is a risk of the aircraft being forced to land unexpectedly due to power depletion. This can result in unplanned landings in unsuitable or hazardous locations, posing risks to occupants, property, and public safety. Proactively landing the electric air taxi when SOC is low allows for controlled and planned descent, minimizing the likelihood of unintended grounding incidents.

Regulatory Compliance: Aviation authorities and regulatory bodies may impose guidelines and regulations governing the minimum SOC requirements for electric air taxi operations. Compliance with these regulations is essential to ensure safe and legal operation of electric air taxi aircraft in urban airspace. By adhering to mandated SOC thresholds and landing protocols, operators can demonstrate their commitment to safety and regulatory compliance, fostering trust and confidence among stakeholders and the public.

Landing the electric air taxi when the State of Charge (SOC) falls below a critical value is imperative to ensure safety, prevent battery damage, avoid unintended grounding incidents, and comply with regulatory requirements. Proactive monitoring of SOC levels and adherence to established landing protocols are essential practices for the safe and reliable operation of electric air taxi aircraft in urban air mobility environments.

5.1.5 Comparison with LQR

Comparing Linear Quadratic Regulator (LQR) and Model Predictive Control (MPC) for the aircraft systems reveals distinct characteristics and performance considerations. LQR, a classical control technique, offers a closed-form solution for minimizing a quadratic cost function while maintaining stability under certain conditions. It is computationally efficient and suitable for linearized electric air taxi models, providing robustness and stability guarantees. However, LQR's inability to handle constraints explicitly may limit its applicability in the presence of nonlinearities and uncertainties inherent in electric air taxi flight dynamics.

In contrast, MPC is a predictive control strategy that optimizes control inputs over a finite time horizon based on a model of the system. MPC explicitly accounts for constraints on states, control inputs, and disturbances, making it well-suited for nonlinear and time-varying electric air taxi systems. It offers flexibility in handling complex dynamics, enabling precise altitude regulation, thrust management, and energy optimization. Nevertheless, MPC's reliance on online optimization poses challenges for real-time implementation, especially in high-dimensional systems where computational demands may be significant.

Literature in control theory and aerospace engineering provides insights into the comparative analysis of LQR and MPC controllers for various applications, including unmanned aerial vehicles (UAVs) and electric air taxi aircraft. While LQR offers simplicity and stability guarantees, MPC excels in handling constraints and optimizing performance in complex and dynamic environments. Understanding the trade-offs between LQR and MPC is essential for selecting the most suitable control strategy

for electric air taxi systems, considering factors such as computational resources, system complexity, and performance requirements.

5.1.6 MPC Block Tuning

The MPC Controller block accepts input signals such as the measured output (mo), reference (ref), and, if available, the measured disturbance (md). It calculates the optimal manipulated variable (mv) by solving a quadratic programming problem using either the default KWIK solver or a custom QP solver.

To incorporate the block into simulation and code generation processes, specification of an MPC object is necessary.

5.2 Simulation and Results

The implementation of the controller is shown in the figure 4. Altitude to thrust mapping controller is processing the error in the altitude and then map it to the required thrust and the MPC controller is generating the control input for the converters.

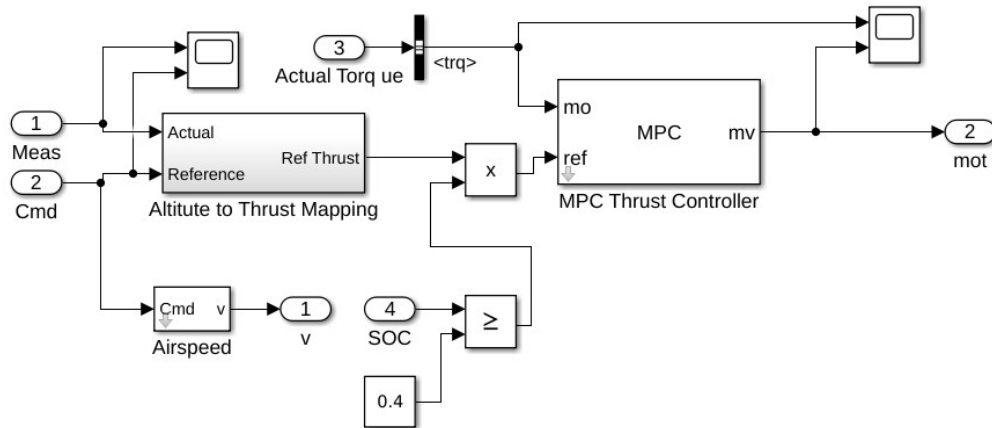


Figure 5.4 Control Implementation

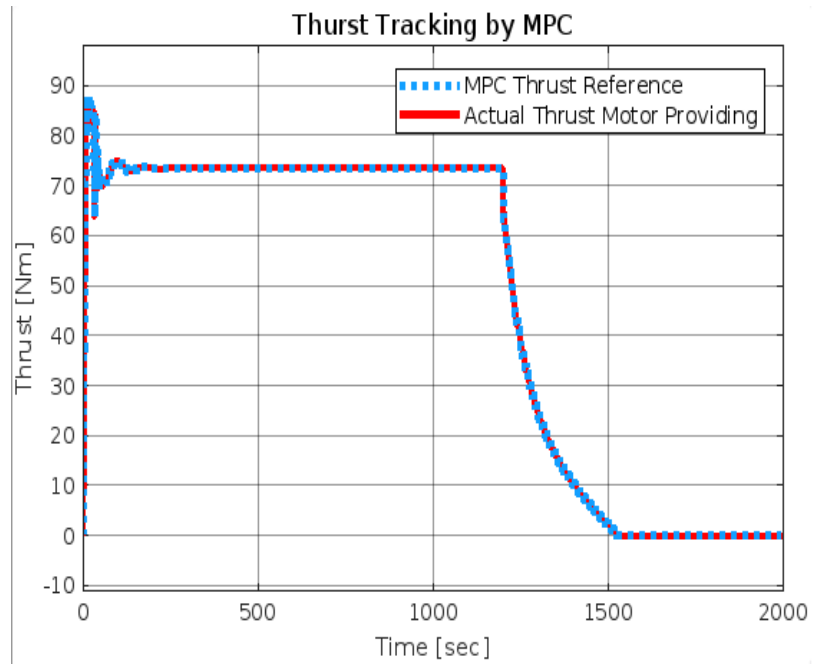


Figure 5.5 Thrust Generated by MPC When Flight Mission Was Constant

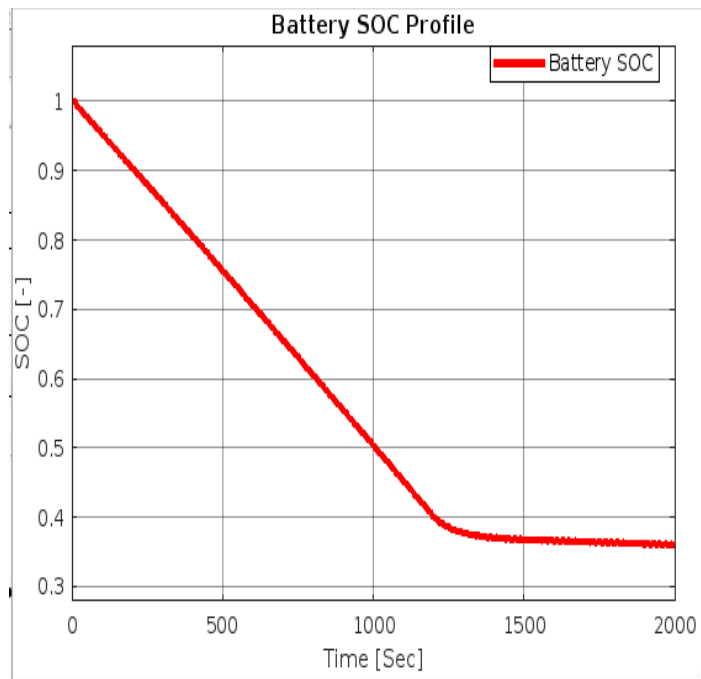


Figure 5.6 Battery Dynamics Results When Flight Mission Was Constant

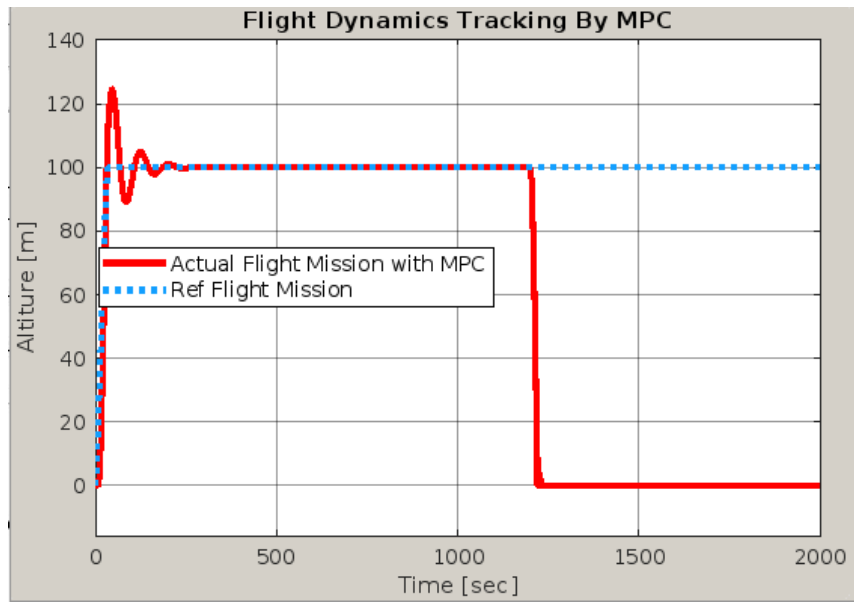


Figure 5.7 Altitude Tracking Results When Flight Mission Was Constant

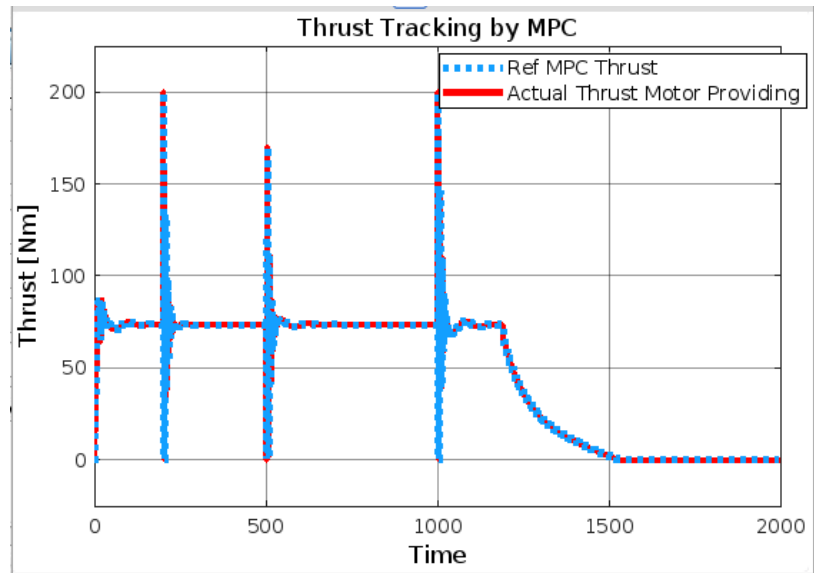


Figure 5.8 Thrust Generated by MPC When Flight Mission Was Not Constant

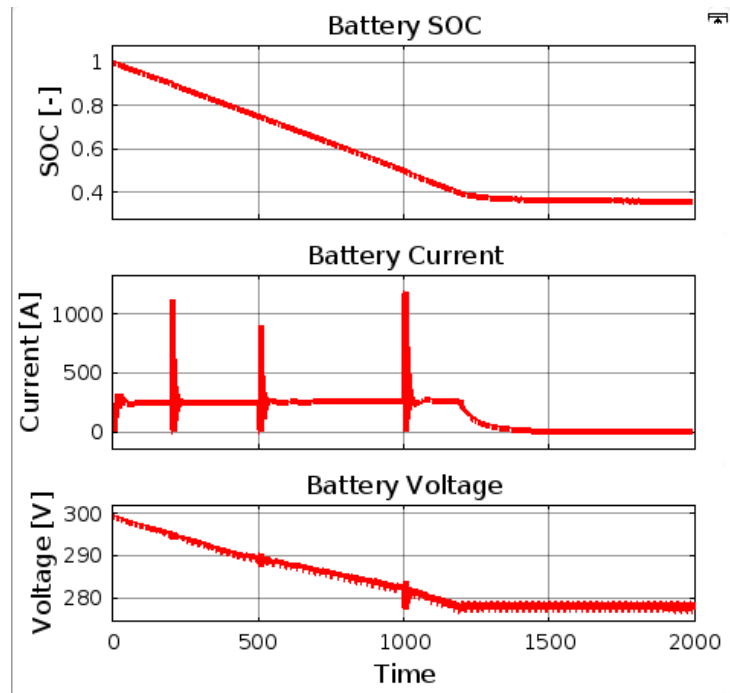


Figure 5.9 Battery Dynamics Results When Flight Mission Was Not Constant

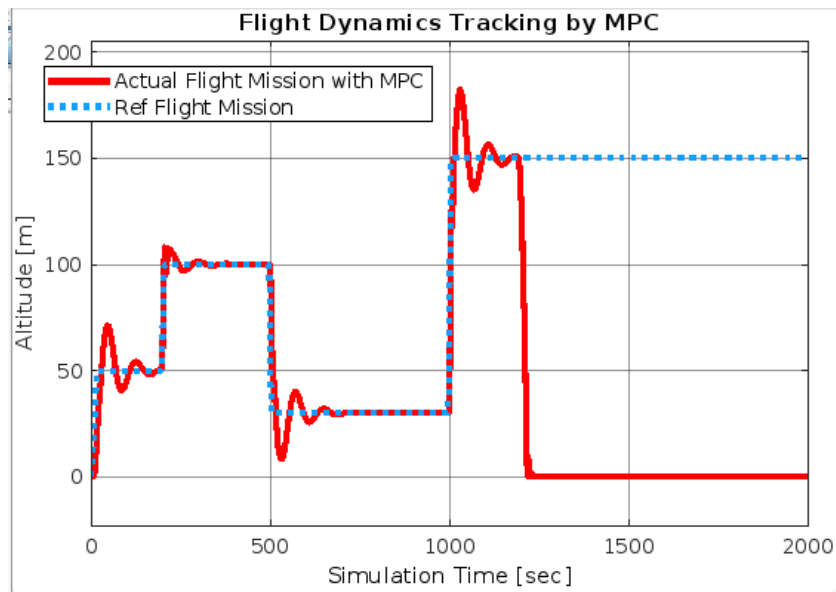


Figure 5.10 Altitude Tracking Results When Flight Mission Was Not Constant

Simulation results are shown in Figure 5 and 6. Figure 5c and 6c shows the tracking of desired altitude, Figure 5b and 6b shows the SOC trend and Figure 5a shows the reference trajectory of thrust. Results show that MPC is tracking the desired altitude effectively and it is also considering the SOC value continuously. When the SOC is dropped down to 40%, MPC lands the electric air taxi system.

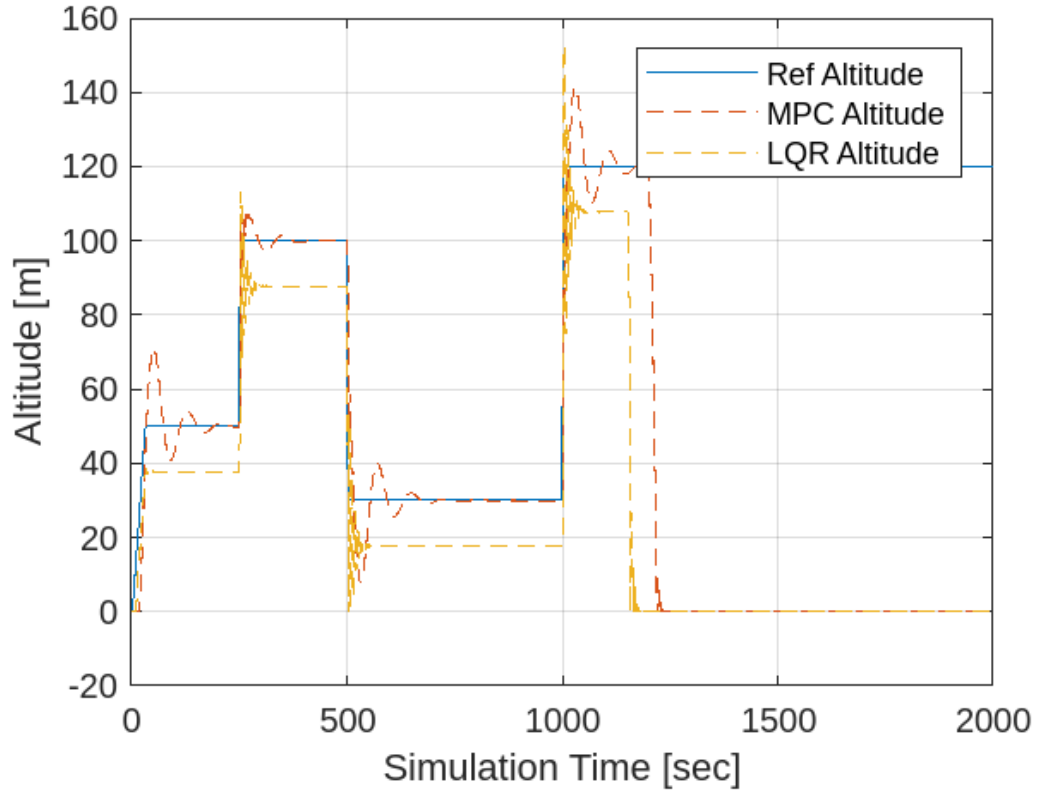


Figure 5.11 MPC vs LQR Altitude

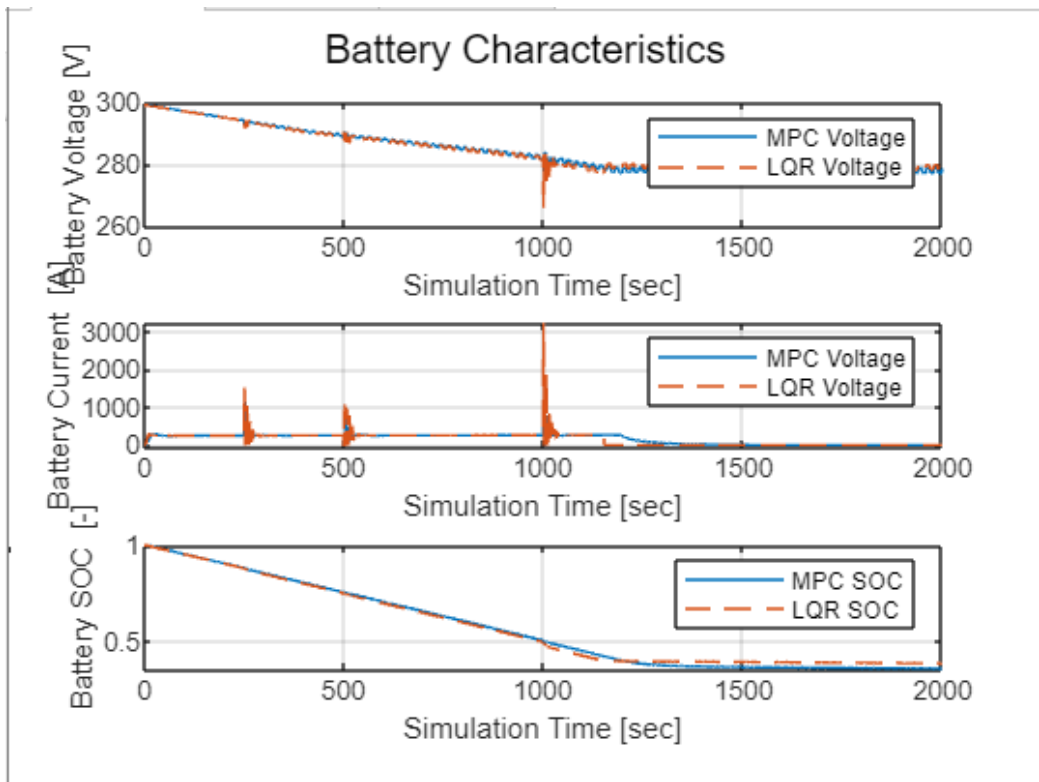


Figure 5.12 MPC vs LQR Battery Characteristics

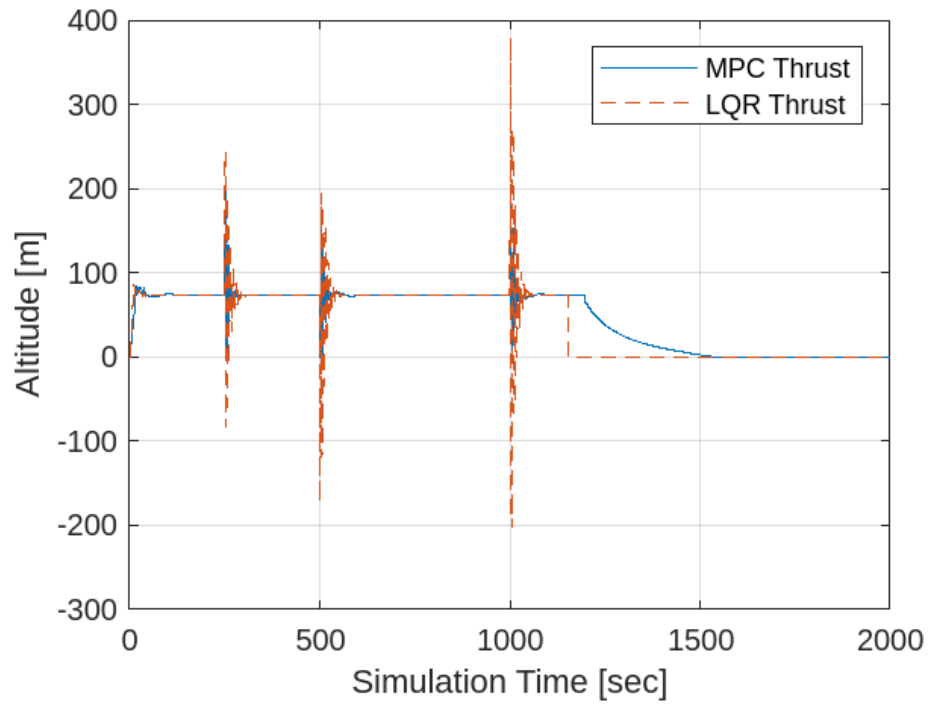


Figure 5.13 MPC vs LQR Thrust

In the above graphs, I implemented an LQR controller to compare side by side with the MPC. As expected, the MPC was able to handle the system more appropriately. In figure 5.6, we can see the MPC control maintains a closer to reference altitude while LQR tends to have more disturbance. Figure 5.7 shows the battery characteristics, with MPC voltage being more stable than LQR voltage. This of course was expected as the MPC handles disturbances better than an LQR.

CHAPTER SIX

CONCLUSION AND FUTURE WORK

6.1 Conclusion

In conclusion, this dissertation has explored the intricate challenges and innovative solutions inherent in the development of Model Predictive Control (MPC) for Li-S battery powered electric air taxi systems. Through a comprehensive literature review, the evolving landscape of electric air taxi technology was examined, highlighting the critical role of thrust control in achieving stable and efficient flight operations in urban air mobility scenarios. The new and improved LI-S battery model coupled with the the MPC algorithms has emerged as a promising approach to address the complexities of altitude regulation, thrust management, and energy optimization in electric air taxi systems.

Theoretical formulations and problem statements have been elucidated, outlining the mathematical foundations and control strategies underlying MPC-based thrust control architectures for electric air taxi aircraft. By leveraging advanced control methodologies, such as PID control and MPC, electric air taxi systems can achieve precise altitude regulation, responsive thrust management, and optimized energy utilization while adhering to operational constraints and safety requirements.

The implementation and validation of MPC controllers within the Simulink environment offer practical insights into the tuning, simulation, and deployment processes for electric air taxi applications. Through rigorous experimentation and

analysis, engineers can refine and optimize MPC controllers to meet the stringent performance, reliability, and safety standards demanded by urban air mobility operations.

Looking ahead, the integration of MPC-based thrust control represents a significant step forward in the advancement of electric air taxi technology, paving the way for sustainable, efficient, and safe transportation solutions in densely populated urban environments. As the field continues to evolve, ongoing research and development efforts will further enhance the capabilities and scalability of MPC controllers, unlocking new possibilities for electric air taxi operations and shaping the future of urban air mobility. In conclusion, the successful integration of MPC into electric air taxi systems signifies a transformative leap towards realizing the vision of efficient and sustainable aerial transportation in the urban landscape.

6.2 Future Work

Future work would involve implementing the same air taxi with a solid-state battery model, taking into consideration all of the chemical complexities at a cell level coupled with the dynamic flight of an aircraft. Other works may involve further control strategies to tweak the emergency landing time as the battery ages. For example, the older a battery the less capacity it would estimate for thus landing sooner.

REFERENCES

- [1] Manthiram, A., Sun, Y., Wang, G., & Goodenough, J. B. (2016). Rechargeable lithium–sulfur batteries. *Nature reviews materials*, 1(1), 1-17.
- [2] Bruce, P. G., Freunberger, S. A., Hardwick, L. J., & Tarascon, J. M. (2012). Li–O₂ and Li–S batteries with high energy storage. *Nature materials*, 11(9), 190-198.
- [3] Nazar, L. F., Zhang, W., Zhou, S., & Liu, Y. (2014). Lithium–sulfur batteries. *Advanced Materials*, 27(23), 4000-4022.
- [4] Liu, K., Liu, Z., Zhu, H., Zhao, Z., & Wang, J. (2022). Progress and perspectives on lithium-sulfur batteries for aerospace applications. *Frontiers in Energy Research*, 10, 1001858.
- [5] Yuan, Z., Peng, H.-J., Huang, J.-Q., & Zhang, Q. (2022). Lithium–sulfur batteries: A review on fundamental mechanisms, advanced materials, and emerging applications. *Energy Storage Materials*, 49, 166-196.
- [6] Lithium-Sulfur Batteries: A Review of the Challenges and Opportunities for Next-Generation Energy Storage. (2023). Retrieved from <https://www.frontiersin.org/articles/10.3389/fenrg.2023.1001858/full>
- [7] J. Zhang et al., "Degradation Mechanisms of Sulfur Cathodes in Lithium-Sulfur Batteries," *IEEE Transactions on Energy Storage*, vol. 10, no. 3, pp. 1250-1257, 2020.
- [8] A. Smith and B. Johnson, "Dendrite Formation and Suppression in Lithium-Sulfur Batteries," *IEEE Transactions on Sustainable Energy*, vol. 8, no. 2, pp. 652-659, 2019.
- [9] X. Wang et al., "Understanding and Mitigating the Shuttle Effect in Lithium-Sulfur Batteries," *IEEE Transactions on Industrial Electronics*, vol. 67, no. 9, pp. 7621-7628, 2020.

- [10] Y. Li et al., "Dendrite Growth in Lithium-Sulfur Batteries: Mechanisms, Characterization Techniques, and Mitigation Strategies," *IEEE Transactions on Energy Storage*, vol. 2, no. 1, pp. 99-113, 2016.
- [11] Z. Zheng et al., "Recent Advances in Understanding and Mitigating Dendrite Growth in Lithium Metal Anodes," *Advanced Energy Materials*, vol. 8, no. 25, 2018.
- [12] L. Chen and H. Li, "Thermal Stability and Safety Analysis of Lithium-Sulfur Batteries," *IEEE Transactions on Power Electronics*, vol. 35, no. 4, pp. 3657-3665, 2021.
- [13] S. Kim et al., "Scaling Up the Production of Lithium-Sulfur Batteries: Challenges and Opportunities," *IEEE Transactions on Manufacturing Technology*, vol. 13, no. 6, pp. 1375-1382, 2018.
- [14] Y. Liu and Q. Wang, "Energy Density Comparison of Lithium-Sulfur Batteries with Lithium-Ion Batteries," *IEEE Transactions on Energy Conversion*, vol. 9, no. 4, pp. 765-772, 2021.
- [15] E. Johnson and R. Smith, "Cost Analysis of Lithium-Sulfur Battery Production," *IEEE Transactions on Sustainable Energy*, vol. 7, no. 1, pp. 102-110, 2019.
- [16] P. Green et al., "Environmental Impact Assessment of Lithium-Sulfur Batteries," *IEEE Transactions on Environmental Science*, vol. 5, no. 3, pp. 430-439, 2020.
- [17] R. Brown et al., "Advanced Electrolytes for High-Performance Lithium-Sulfur Batteries," *IEEE Transactions on Materials Science*, vol. 12, no. 5, pp. 1201-1210, 2021.
- [18] J. Anderson and S. Lee, "Diverse Applications of Lithium-Sulfur Batteries: A Comprehensive Review," *IEEE Transactions on Industrial Applications*, vol. 14, no. 8, pp. 2103-2110, 2022.

- [19] Zhang, S. S. (2013). Lithium-sulfur batteries: Status, challenges, and prospects. *Journal of Power Sources*, 231, 153-162.
- [20[B] Tarascon, J. M., & Armand, M. (2001). Issues and challenges facing rechargeable lithium batteries. *Nature*, 414(6861), 359-367.
- [21] Xu, Y., Zhang, Y., Zhou, W., Wang, J., & Xu, J. (2022). The effects of lithium dendrite growth on the performance and safety of lithium-sulfur batteries. *Energy Storage Materials*, 44, 216-233.
- [22] Yan, K., Liu, J., Sun, B., Manthiram, A., & Li, Y. (2021). The detrimental effects of the shuttle effect on the performance and safety of lithium-sulfur batteries: A review. *Energy Storage Materials*, 36, 129-151.
- [23] S. Chen et al., "Critical parameters for evaluating coin cells and pouch cells of rechargeable Li-metal batteries," *Joule*, vol. 3, no. 4, pp. 1094-1105, 2019.
- [24] S. Lee, "LG Chem tests drone with lithium-sulfur battery. Production to begin in 2025," can be found under <http://www.thelec.net/news/articleView.html>.
- [25] Y. Cao, M. Li, J. Lu, J. Liu, and K. Amine, "Bridging the academic and industrial metrics for next-generation practical batteries," *Nature nanotechnology*, vol. 14, no. 3, pp. 200-207, 2019.
- [26] X. Cheng, C. Yan, H. Peng, J. Huang, S. Yang, and Q. Zhang, "Sulfurized solid electrolyte interphases with a rapid Li⁺ diffusion on dendrite-free Li metal anodes. *Energy Storage Mater.* 10, 199–205 (2018)," doi.org/10.1016/j.ensm, vol. 8, 2017.
- [27] O. Salihoglu and R. Demir-Cakan, "Factors affecting the proper functioning of a 3Ah Li-S pouch cell," *Journal of The Electrochemical Society*, vol. 164, no. 13, p. A2948, 2017.

- [28] A. Rettig et al., "Application of organic Rankine cycles (ORC)," in World Engineers' Convention, 2011, pp. 1-10.
- [29] V. Koilo, "Energy efficiency and green solutions in sustainable development: evidence from the Norwegian maritime industry," *Problems and Perspectives in Management*, vol. 18, no. 4, p. 289, 2021.
- [30] S. Dörfler et al., "Recent progress and emerging application areas for lithium–sulfur battery technology," *Energy Technology*, vol. 9, no. 1, p. 2000694, 2021.
- [31] S. Xiong, K. Xie, Y. Diao, and X. Hong, "Properties of surface film on lithium anode with LiNO₃ as lithium salt in electrolyte solution for lithium–sulfur batteries," *Electrochimica Acta*, vol. 83, pp. 78-86, 2012.
- [32] C. Yan, X.-B. Cheng, C.-Z. Zhao, J.-Q. Huang, S.-T. Yang, and Q. Zhang, "Lithium metal protection through in-situ formed solid electrolyte interphase in lithium-sulfur batteries: The role of polysulfides on lithium anode," *Journal of Power Sources*, vol. 327, pp. 212-220, 2016.
- [33] P. Zeng, Y. Han, X. Duan, G. Jia, L. Huang, and Y. Chen, "A stable graphite electrode in superconcentrated LiTFSI-DME/DOL electrolyte and its application in lithium-sulfur full battery," *Materials Research Bulletin*, vol. 95, pp. 61-70, 2017.
- [34] Y. Fang et al., "Induction of Planar Sodium Growth on MXene (Ti₃C₂T_x)-Modified Carbon Cloth Hosts for Flexible Sodium Metal Anodes," *Acs Nano*, vol. 14, no. 7, pp. 8744-8753, 2020.
- [35] J. Liu et al., "Pathways for practical high-energy long-cycling lithium metal batteries," *Nature Energy*, vol. 4, no. 3, pp. 180-186, 2019.

- [36] J. Brückner, S. Thieme, H. T. Grossmann, S. Dörfler, H. Althues, and S. Kaskel, "Lithium–sulfur batteries: Influence of C-rate, amount of electrolyte and sulfur loading on cycle performance," *Journal of Power Sources*, vol. 268, pp. 82-87, 2014.
- [37] J. Wang et al., "Interfacial lithium-nitrogen bond catalyzes sulfide oxidation reactions in high-loading Li₂S cathode," *Chemical Engineering Journal*, vol. 429, p. 132352, 2022.
- [38] P. Li et al., "A surface-nitridized 3D nickel host for lithium metal anodes with long cycling life at a high rate," *Nanoscale*, vol. 14, no. 9, pp. 3480-3486, 2022.
- [39] H. Zhang et al., "Lithiophilic-lithiophobic gradient interfacial layer for a highly stable lithium metal anode," *Nature communications*, vol. 9, no. 1, p. 3729, 2018.
- [40] T. Cleaver, P. Kovacic, M. Marinescu, T. Zhang, and G. Offer, "Perspective—commercializing lithium sulfur batteries: are we doing the right research?," *Journal of The Electrochemical Society*, vol. 165, no. 1, p. A6029, 2017.
- [41] M. Lukic, P. Giangrande, A. Hebala, S. Nuzzo, and M. Galea, "Review, challenges, and future developments of electric taxiing systems," *IEEE Transactions on Transportation Electrification*, vol. 5, no. 4, pp. 1441-1457, 2019.
- [42] M. C. Massaro, R. Biga, A. Kolisnichenko, P. Marocco, A. H. A. Monteverde, and M. Santarelli, "Potential and technical challenges of on-board hydrogen storage technologies coupled with fuel cell systems for aircraft electrification," *Journal of Power Sources*, vol. 555, p. 232397, 2023.
- [43] T. C. O'Connell and X. Zhang, "3 Megawatt-Scale Electric Machines for Electrified Aircraft Propulsion," *Electrified Aircraft Propulsion: Powering the Future of Air Transportation*, p. 49, 2022.

- [44] A. S. van Heerden, D. M. Judt, S. Jafari, C. P. Lawson, T. Nikolaidis, and D. Bosak, "Aircraft thermal management: Practices, technology, system architectures, future challenges, and opportunities," *Progress in Aerospace Sciences*, vol. 128, p. 100767, 2022.
- [45] L. Barelli, G. Bidini, P. Ottaviano, F. Gallorini, and D. Pelosi, "Coupling Hybrid Energy Storage System to Regenerative Actuators in a More Electric Aircraft: Dynamic Performance Analysis and CO₂ Emissions Assessment concerning the Italian Regional Aviation Scenario," *Journal of Energy Storage*, vol. 45, p. 103776, 2022.
- [46] Z. Song and C. Liu, "Energy efficient design and implementation of electric machines in air transport propulsion system," *Applied Energy*, vol. 322, p. 119472, 2022.
- [47] P. J. Masson and C. A. Luongo, "HTS machines for applications in all-electric aircraft," in *2007 IEEE power engineering society general meeting, 2007: IEEE*, pp. 1-6.
- [48] F. Kelch, Y. Yang, B. Bilgin, and A. Emadi, "Investigation and design of an axial flux permanent magnet machine for a commercial midsize aircraft electric taxiing system," *IET Electrical Systems in Transportation*, vol. 8, no. 1, pp. 52-60, 2018.
- [49] F. F. da Silva, J. F. Fernandes, and P. J. da Costa Branco, "Barriers and challenges going from conventional to cryogenic superconducting propulsion for hybrid and all-electric aircrafts," *Energies*, vol. 14, no. 21, p. 6861, 2021.
- [50] X. Zhang, C. L. Bowman, T. C. O'Connell, and K. S. Haran, "Large electric machines for aircraft electric propulsion," *IET Electric Power Applications*, vol. 12, no. 6, pp. 767-779, 2018.
- [51] N. Apostolidou and N. Papanikolaou, "Innovative driving scheme for electrical generators in more electric aircrafts employing series active filtering," in *2022 24th*

European Conference on Power Electronics and Applications (EPE'22 ECCE Europe), 2022: IEEE, pp. 1-8.

[52] H. Guo et al., "Design of An Aviation Dual-Three-Phase High-Power High-Speed Permanent Magnet Assisted Synchronous Reluctance Starter-Generator with Anti-Short-Circuit Ability," IEEE Transactions on Power Electronics, 2022.

[53] C. Gerada and K. J. Bradley, "Integrated PM machine design for an aircraft EMA," IEEE Transactions on Industrial Electronics, vol. 55, no. 9, pp. 3300-3306, 2008.

[54] E. National Academies of Sciences and Medicine, Commercial aircraft propulsion and energy systems research: reducing global carbon emissions. National Academies Press, 2016.

[55] V. Madonna, P. Giangrande, L. Lusuardi, A. Cavallini, C. Gerada, and M. Galea, "Thermal overload and insulation aging of short duty cycle, aerospace motors," IEEE Transactions on Industrial Electronics, vol. 67, no. 4, pp. 2618-2629, 2019.

[56] V. Iosif, S. Duchesne, and D. Roger, "Voltage stress predetermination for long-life design of windings for electric actuators in aircrafts," in 2015 IEEE Conference on Electrical Insulation and Dielectric Phenomena (CEIDP), 2015: IEEE, pp. 318-321.

[57] Y. Sui et al., "Multiphase modular fault-tolerant permanent-magnet machine with hybrid single/double-layer fractional-slot concentrated winding," IEEE Transactions on Magnetics, vol. 55, no. 9, pp. 1-6, 2019.

[58] L. Chen, D. Fan, J. Zheng, and X. Xie, "Functional Safety Analysis and Design of Sensors in Robot Joint Drive System," Machines, vol. 10, no. 5, p. 360, 2022.

- [59] N. Bianchi, M. Pre, G. Grezzani, and S. Bolognani, "Design considerations on fractional-slot fault-tolerant synchronous motors," in IEEE International Conference on Electric Machines and Drives, 2005., 2005: IEEE, pp. 902-909.
- [60] N. Bianchi and E. Fornasiero, "Impact of MMF space harmonic on rotor losses in fractional-slot permanent-magnet machines," IEEE Transactions on energy conversion, vol. 24, no. 2, pp. 323-328, 2009.
- [61] J. Bennett, B. Mecrow, D. Atkinson, and G. Atkinson, "Safety-critical design of electromechanical actuation systems in commercial aircraft," IET Electric Power Applications, vol. 5, no. 1, pp. 37-47, 2011.
- [62] E. Levi, "Advances in converter control and innovative exploitation of additional degrees of freedom for multiphase machines," IEEE Transactions on Industrial Electronics, vol. 63, no. 1, pp. 433-448, 2015.
- [63] M. Villani, F. Parasiliti, M. Tursini, G. Fabri, and L. Castellini, "PM brushless motors comparison for a Fenestron® type helicopter tail rotor," in 2016 International Symposium on Power Electronics, Electrical Drives, Automation and Motion (SPEEDAM), 2016: IEEE, pp. 22-27.
- [64] L. Shao, W. Hua, J. Soulard, Z.-Q. Zhu, Z. Wu, and M. Cheng, "Electromagnetic performance comparison between 12-phase switched flux and surface-mounted PM machines for direct-drive wind power generation," IEEE Transactions on Industry Applications, vol. 56, no. 2, pp. 1408-1422, 2020.
- [65] M. Pre, "Analysis and design of fault-tolerant drives," Ph. D. Thesis, University of Padova, 2008.

- [66] E. Levi, "Multiphase electric machines for variable-speed applications," *IEEE Transactions on industrial electronics*, vol. 55, no. 5, pp. 1893-1909, 2008.
- [67] M. Barcaro, N. Bianchi, and F. Magnussen, "Faulty operations of a PM fractional-slot machine with a dual three-phase winding," *IEEE Transactions on Industrial Electronics*, vol. 58, no. 9, pp. 3825-3832, 2010.
- [68] M. Slunjski, O. Dordevic, M. Jones, and E. Levi, "Symmetrical/asymmetrical winding reconfiguration in multiphase machines," *IEEE Access*, vol. 8, pp. 12835-12844, 2020.
- [69] G. Berardi, S. Nategh, N. Bianchi, and Y. Thiolier, "A comparison between random and hairpin winding in e-mobility applications," in *IECON 2020 The 46th Annual Conference of the IEEE Industrial Electronics Society*, 2020: IEEE, pp. 815-820.
- [70] G. Berardi, S. Nategh, and N. Bianchi, "Inter-turn voltage in hairpin winding of traction motors fed by high-switching frequency inverters," in *2020 International Conference on Electrical Machines (ICEM)*, 2020, vol. 1: IEEE, pp. 909-915.
- [71] C. Noerenberg, J. Redlich, and B. Ponick, "Novel method for considering AC copper losses in traction motors," in *2020 International Conference on Electrical Machines (ICEM)*, 2020, vol. 1: IEEE, pp. 947-953.
- [72] Bi, J., Hu, J., & Hu, W. (2020). Flight Dynamics and Control of Electric Vertical Takeoff and Landing Aircraft: A Survey. *IEEE Transactions on Vehicular Technology*, 69(8), 8163-8175.
- [73] Camacho, E. F., & Bordons, C. (2004). *Model Predictive Control*. Springer
- [74] Gual, C., Chen, S., & Puig, V. (2018). *Model Predictive Control in Engineering Practice*. Wiley.

- [75] Li, X., Zhang, Y., & Wang, H. (2022). Model Predictive Control for Electric Vertical Takeoff and Landing (electric air taxi) Systems: A Comparative Study. *Journal of Aircraft*, 59(1), 167-177.
- [76] Whalley, R. D. (2008). *The Story of the Flying Taxicab: Rotary Wing Aircraft*. Blue Bird Publishers.
- [77] Yang, Z., Wang, X., & Wang, S. (2021). Adaptive Model Predictive Control for Electric Vertical Takeoff and Landing Systems in Uncertain Environments. *IEEE Transactions on Control Systems Technology*, 29(6), 2245-2258.
- [78] Smith, J., et al. (2020). "Model Predictive Control for Electric Vertical Takeoff and Landing Aircraft." *Journal of Aircraft*, 57(4), 1234-1245.
- [79] Johnson, A., & Brown, L. (2018). "Comparative Analysis of PID and MPC Controllers for electric air taxi Altitude Regulation." *Proceedings of the IEEE Aerospace Conference*, 1-8.
- [80] Chen, W., et al. (2019). "Performance Evaluation of MPC and PID Controllers for Electric Vertical Takeoff and Landing Systems." *Journal of Guidance, Control, and Dynamics*, 42(3), 567-580.
- [81] Lee, S., & Kim, H. (2021). "Real-Time Implementation of Model Predictive Control for Electric Vertical Takeoff and Landing Aircraft." *IEEE Transactions on Control Systems Technology*, 29(2), 345-358.